

Performance Evaluation of an IEEE 802.15.4 Sensor Network with a Star Topology[†]

Chandramani Kishore Singh[‡], Anurag Kumar[‡], and P. M. Ameer[‡]

Abstract—One class of applications envisaged for the IEEE 802.15.4 LR-WPAN (low data rate - wireless personal area network) standard is wireless sensor networks for monitoring and control applications. In this paper we provide an analytical performance model for a network in which the sensors are at the tips of a star topology, and the sensors need to transmit their measurements to the hub node so that certain objectives for packet delay and packet discard are met.

We first carry out a saturation throughput analysis of the system; i.e., it is assumed that each sensor has an infinite backlog of packets and the throughput of the system is sought. After a careful analysis of the CSMA/CA MAC that is employed in the standard, and after making a certain decoupling approximation, we identify an embedded Markov renewal process, whose analysis yields a fixed point equation, from whose solution the saturation throughput can be calculated. We validate our model against ns2 simulations (using an IEEE 802.15.4 module developed by J. Zheng [14]). We find that with the default back-off parameters the saturation throughput decreases sharply with increasing number of nodes. We use our analytical model to study the problem and we propose alternative back-off parameters that prevent the drop in throughput.

We then show how the saturation analysis can be used to obtain an analytical model for the finite arrival rate case. This finite load model captures very well the qualitative behavior of the system, and also provides a good approximation to the packet discard probability, and the throughput. For the default parameters, the finite load throughput is found to first increase and then decrease with increasing load. We find that for typical performance objectives (mean delay and packet discard) the packet discard probability would constrain the system capacity. Finally, we show how to derive a node lifetime analysis using various rates and probabilities obtained from our performance analysis model.

Keywords: wireless sensor networks, performance analysis, LR-WPANs

I. INTRODUCTION

Low rate-wireless personal area networks (LR-WPANs) are designed to serve a variety of applications with a focus on enabling wireless sensor networks. The IEEE 802.15.4 standard [1] has evolved to realize the physical (PHY) and multiple access control (MAC) layers of such LR-WPANs. The ZigBee alliance has developed the network and upper layers [2]. The overall objective of our work reported here is to analyse the performance of such networks for industrial sensing and measurement applications. The aim is to replace existing wired sensor networks (based, e.g., on the Fieldbus

standard) with wireless ad hoc sensor networks. The end to end applications, however, will initially remain unchanged. Hence the concern is whether the wireless network will be able to carry the measurement traffic with the same level of performance as the wired network.

A. Preview of Contributions

In this paper we provide the results of our analysis of a star topology sensor network based on the IEEE 802.15.4 standard. Here we limit our work to the situation in which packets flow only from the sensors to the head of the hub of the star (i.e., the PAN coordinator). We first obtain the saturation throughput of the network. Then we provide some results on performance with finite rate arrivals of measurements. The following is a preview of our main contributions and findings.

- 1) We provide a fixed point analysis, using a decoupling approximation (see [4] and [10]) for the saturation throughput analysis of IEEE 802.15.4 networks. The CSMA/CA mechanism in IEEE 802.15.4 is significantly different from that in IEEE 802.11, for which the analyses in [4] and [10] were done. Hence a major novelty in our present work is that we extract a Markov renewal process model for the evolution of the CSMA/CA channel in IEEE 802.15.4, and then develop a decoupling approximation for this model. We find that our analysis captures the saturation throughput with a maximum error of 5% (see Figure 16).
- 2) We find that the design of the CSMA/CA MAC in IEEE 802.15.4 is such that the aggregate saturation throughput decreases sharply with the number of nodes. We use our analytical model to show that with the default parameters, with increasing number of nodes the backoff adaptation does not work well and the network operates in a congested regime. We show that, staying within the framework of the standard, it is possible to modify the backoff parameters so that the saturation throughput decreases only slightly when the number of nodes increases. It is also found that packet discard probability is much reduced after these modifications (see Figures 18 and 19).
- 3) The saturation analysis thus obtained is used to perform a heuristic finite load analysis. Simulations show that the analysis captures very well the qualitative behaviour of delay, throughput, and packet discard probabilities, and for the latter two also provides a good analytical approximation (see Figures 21 and 22).
- 4) Finally, we show how a node lifetime analysis can be

[†]The work was sponsored by the Honeywell Technology Solutions Lab., Bangalore, India.

[‡]Department of Electrical Communication Engg., Indian Institute of Science, Bangalore, 560 012, INDIA; email: cksingh, anurag, ameer@ece.iisc.ernet.in

performed by using the various event rates and probabilities derived from our performance analysis model (see Figure 23).

B. Related Literature

Zheng and Lee [11] have given an overview of the standard. Kinney [9] has provided a description of ZigBee technology, along with a comparative study of ZigBee with Bluetooth. There have been several simulation studies of the IEEE 802.15.4 CSMA/CA mechanism. In [15], Zheng and Lee report on a module that they have developed for the ns2 simulator ([14]), and provide results from several sets of simulation experiments. Other simulation studies have been reported in [25], [12], [7]. Timmons and Scanlon have done the very first analytical modeling of the IEEE 802.15.4 single cell network in the context of medical sensor body area networks. Their much simplified analysis [13] focuses on long-term power consumption of devices. Park et al. [19], Pollin et al. [18], and Tao et al. [21] propose Markov chain models to analyse the performance of the 802.15.4 slotted CSMA/CA protocol in the saturation condition. The analytical approach is similar to that introduced by Bianchi [4] for analysing the IEEE 802.11 DCF with saturated nodes. In [21], the authors assume that times at which channel activity starts are renewal instants, and develop a 3-dimensional Markov chain for the joint evolution of a node's back-offs and the residual time within a channel cycle. This yields a complex Markov chain, whose transition probabilities are expressed in terms of an unknown vector of probabilities. Finally, after some assumptions the analysis involves the solution of a vector fixed point equation in this unknown vector of probabilities. One assumption that is made is that the number of nodes that can attempt at any time is always n , the total number of nodes. Also, only saturation analysis is performed. In [22], Ramachandran et al. model the contention access period specified in the IEEE 802.15.4 standard using nonpersistent CSMA as the access mechanism. The authors show that reducing the number of CCAs to 1 is advantageous in terms of achievable throughput and delay in situations where a MAC layer acknowledgment is not required. The analysis is also based on a Markov chain model for the behaviour of each node, but is limiting since no buffering at the nodes is considered. The authors replace the uniform distribution of backoff window size with a geometric distribution of the same mean. The possibility of collisions is ignored while formulating the Markov chain model of a tagged node. In [17] the authors consider a beacon enabled star topology network with bidirectional traffic. Each node is modeled as an M/G/1 queue and then a Markov model like the one developed by Bianchi [4] is obtained.

Kohvakka et al. in [16] provide a simplified analysis of a cluster tree topology of IEEE 802.15.4 sensor nodes. Leibnitz et al. [20] report the analysis of IEEE 802.15.4 CSMA/CA when all nodes initiate their transmission attempts simultaneously. Thus these authors do not consider any particular traffic model. Koubaa et al. [24], discuss the inefficiencies of the CFP and GTS mechanisms of IEEE 802.15.4 standard. The authors then propose an implicit GTS allocation mechanism

(i-GAME) to address the problems observed. Ramachandran [23] has reported a comprehensive list of bugs in the existing ns2 implementation of 802.15.4.

In our work we have followed an approach along the lines of Kumar et al. [10]. We first obtain a saturation analysis in which each node is characterised by a single unknown attempt probability, which is obtained by the solution of a fixed point equation. Then a finite load analysis is obtained by a novel application of the saturation analysis. Overall the analysis is simpler than the one based on detailed per node Markov chains and provides better insight. Also we compare our results against the more standard ns2 simulator.

C. Outline of the paper

The rest of the paper is organized as follows. Section II briefly reviews LR-WPAN architecture and its specifications. In Section III we identify various scenarios that occur when nodes interact using the IEEE 802.15.4 slotted CSMA/CA MAC. In Section V, we identify a cyclic evolution of system behaviour, provide a stochastic model of the evolution of certain processes, and also formulate a fixed point equation. Various performance measures are derived in Section VI. Numerical results along with a discussion are also provided in the same chapter. In Section VII-B, we discuss how back-off parameters can be changed to modify network performance. In Section VIII we use the saturation analysis to develop a finite load analysis. In Section IX we show how our model can be used to derive an estimate of node lifetime. Finally Section X we summarise the insights gained from our work in this paper. The appendix contains the details of the derivations of various transition probabilities and conditional distributions.

II. IEEE 802.15.4: A SHORT OVERVIEW AND SCOPE OF OUR MODELING

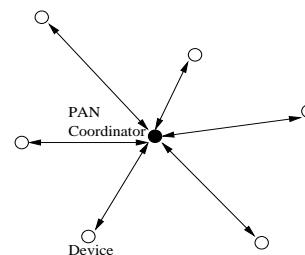


Fig. 1. A star topology LR-WPAN sensor network

We begin by providing a quick overview of the parts of the IEEE 802.15.4 MAC standard that are relevant to our study. Figure 1 shows a star topology sensor network comprising a PAN coordinator and several sensors as leaf nodes. Since we consider only a simple star topology, with flow of traffic only from the leaf nodes to the hub, we need to consider only the PHY and MAC standards.

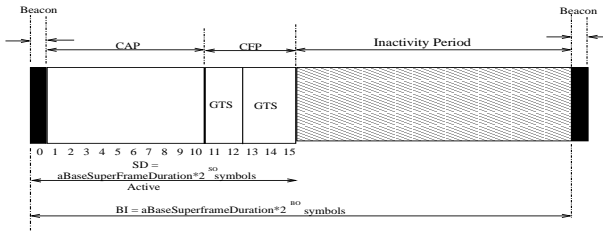


Fig. 2. The IEEE 802.15.4 superframe structure.

A. PHY and MAC Overview

Throughout we assume that we are working in the 2.45GHz band and hence the PHY data rate is 250 Kbps, the symbol rate is 62.5 symbols/second; hence the symbol time is $16\mu\text{s}$. In practice wireless transceivers are always half duplex. Hence the IEEE 802.15.4 devices require a finite amount of time to switch between transmission and reception. This time is denoted by $aTurnaroundTime$ in the standard and is equal to 12 symbol times.

We now turn to the MAC specifications. The IEEE 802.15.4 can operate either in a beacon enabled or a non-beacon enabled mode. In the beacon enabled mode, the PAN coordinator works with time slots defined through a superframe structure (see Figure 2). This permits a synchronous operation of the network so that nodes can go to sleep and wake up at designated times. We assume this mode in our work. Each superframe has active and inactive portions. The PAN Coordinator interacts with the network only during the active portion. The active portion is composed of three parts: a beacon, a contention access period (CAP), and a contention free period (CFP). The active portion starts with the transmission of a beacon and a CAP commences immediately after the beacon. All frames, except acknowledgment frames and any data frame that immediately follows the acknowledgment of a data request command (as would happen following a data request from a node to the PAN coordinator), transmitted in the CAP, must use a slotted CSMA/CA mechanism to access the channel. We note that we do not model data requests from nodes to the PAN coordinator in our work reported here.

The CFP, if present, follows immediately after the CAP and extends up to the end of the active portion of the superframe (see Figure 2). To use a CFP, a node issues an explicit GTS (guaranteed time slot) allocation request to the PAN coordinator. The PAN coordinator, can allocate available GTSs to nodes. In the CFP, a device can transmit during its GTS, without any contention with other devices. We note that, as per the standard, the PAN coordinator may allocate only up to seven GTSs in a CFP. Hence, no more than seven nodes can be involved in the CFP during a superframe. It follows that in a network with a large number of nodes this feature will be useful only for sporadic alarm traffic that requires very low latency. See also [24] for an additional discussion of the limitations of the GTS mechanism.

Transmitted frames are always followed by an IFS period. Frames (MPDUs) of length up to $aMaxSIFSFrameSize$ are followed by a SIFS period of duration of at least $aMinSIF-$

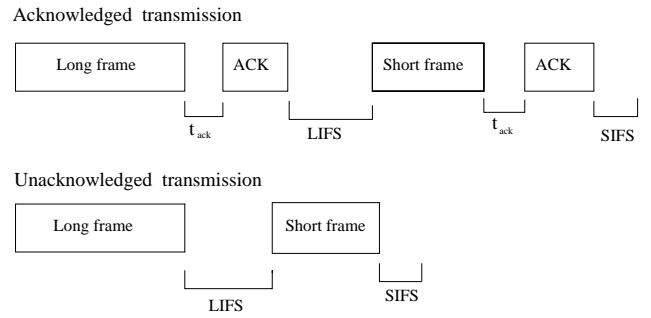


Fig. 3. Illustration of LIFS and SIFS

$SPeriod$ symbols, otherwise a LIFS of a duration at least $aMinLIFSPeriod$ symbols follows (see Figure 3).

B. Scope of Our Analytical Model

We consider a beacon enabled star topology network, in which all the communication is from the sensors to the PAN coordinator. Thus we do not consider peer-to-peer communication, nor do we consider mesh topologies. We only model the slotted CSMA/CA MAC, and not unslotted CSMA/CA.

Since we are interested in an application in which measurements continuously flow from the sensors to the PAN coordinator, it is assumed that the active part of the superframe is equal to the beacon interval. For such traffic the time reserved in the CFP part of a superframe will often be wasted. Thus, no CFPs are assumed¹. Since we focus on analyzing the performance of slotted CSMA/CA, we assume a large superframe duration. This allows us to ignore the beacon transmission time and all the time wasted at the end of each beacon interval due to nodes not being able to complete their transmissions in the fragment of time left at the end of a beacon interval. Thus all of channel time is assumed to be used for CSMA/CA based access.

Since we are analyzing the star topology, which has only one hop transmissions, the ZigBee routing algorithm does not come into the picture. It is also assumed that none of the devices disassociates during the whole traffic flow, and also that communication failures never cause a device to conclude that it has been orphaned.

We assume also that all nodes are perfectly synchronized at backoff period boundaries.

C. The Slotted CSMA/CA Algorithm

The CSMA/CA algorithm is implemented using units of time, called backoff periods, each of length $aUnitBackoffPeriod$ ($= 20$ symbol times $= 0.32$ ms). Note that 10 bytes can be transmitted in one backoff period. In slotted CSMA/CA, the backoff period boundaries of every device in the PAN are aligned with the superframe slot boundaries of the PAN coordinator, and transmissions begin on the boundary of a backoff period.

¹We note that the CSMA/CA mechanism can be analysed in the presence of the GTS mechanism by using an approach based on queues with service interruptions (see [3]).

Each device maintains three variables for each transmission attempt: NB, CW and BE. NB is initialised to 0, and counts the number of additional backoffs the algorithm has to do while attempting the current transmission. CW is the number of backoff periods, that need to be clear of channel activity before the transmission can commence. MAC ensures this by performing *clear channel assessment* (CCA) at the boundary of CW consecutive backoff periods². CW is set to 2 before each transmission attempt, i.e., two consecutive CCAs must find the channel clear in order for the node to attempt a transmission. BE is the backoff exponent and is initialized to *macMinBE*. If a node finds a packet at the head-of-line (HOL) of its buffer, it starts a backoff uniformly distributed over $(0, 2^{BE} - 1)$ backoff periods. The backoff counter is decremented by 1 at the start boundaries of successive backoff periods irrespective of any channel activity. The counter is frozen during the CFP and the inactive portion of a superframe, and resumes when the CAP in the following superframe begins. Once the backoff counter reaches 0, the node starts performing CCAs. If both the CCAs succeed, the node transmits the packet. If either of the CCAs fails, CW is reset to two and both NB and BE are increased by one, ensuring that BE does not exceed *aMaxBE*. If the value of NB is greater than *macMaxCSMABackoff*, the CSMA/CA algorithm terminates with a Channel Access Failure status. The packet being attempted is discarded after a Channel Access Failure. If both the CCAs from a node succeed, it proceeds to transmit the HOL packet, provided that the frame transmission and the subsequent acknowledgment can be completed one IFS period before the end of the CAP. If this is not possible, the node shall defer its transmission until the start of the CAP of the following superframe.

If the node can proceed, it transmits the packet. This may result either in a successful transmission or a collision. A successful transmission is always accompanied by the reception of a MAC acknowledgment. A MAC acknowledgment is of fixed length, 11 bytes. The transmitting node always waits for acknowledgment for *macAckWaitDuration* before declaring a collision. If the packet collides with some other packet while being transmitted, it is retransmitted with all backoff parameters set to their initial values. A packet is retransmitted at most *aMaxFrameRetries* times after transmission failures due to collisions, before being discarded.

CSMA/CA employs one more parameter *macBattLifeExt* to exploit the possibility of energy savings at the PAN coordinator in case of very low duty-cycle traffic. In slotted systems with *macBattLifeExt* set to TRUE, the backoff countdown only occurs during the first *macBattLifeExtPeriods* full backoff periods following the beacon. An IFS period and subsequent frame transmissions to the PAN Coordinator are required to start in this duration. So if the PHY at the PAN Coordinator does not indicate any reception during this period, the PAN Coordinator can go into a doze mode, thus saving its battery energy. If

macBattLifeExt is set to TRUE, the backoff exponent BE is initialized to the smaller of 2 and *macMinBE*; otherwise BE is initialised to *macMinBE*.

The CSMA/CA algorithm analysed in this paper assumes *macBattLifeExt* set to FALSE, so that backoff countdown can occur throughout the active portion of the superframe and the frame transmission also can start at any of the backoff period boundaries throughout the active portion of the superframe.

The default values of the various CSMA/CA parameters, as in the standard, are given in the following table.

Parameter	Value
aMaxBE	5
aMaxframeRetries	3
macMaxCSMABackoffs	4
macMinBE	3
macBattLifeExt	FALSE

III. UNDERSTANDING NODE INTERACTIONS IN THE IEEE 802.15.4 SLOTTED CSMA/CA ALGORITHM

Our first aim is to develop an analytical model for calculating the saturation throughput of an IEEE 802.15.4 star network. By saturation throughput it is meant that all the nodes always have packets to send, and hence always contend for access. Saturation throughput is one measure of system capacity, and we will see how it can be used to develop an approximate analysis for finite arrival rates.

Like all such standards, the IEEE 802.15.4 MAC standard [1] is written with an implementer in mind. *It describes the behaviour of an individual node.* In order to model the system, however, *we need to understand how nodes interact.* In this section we will identify the various scenarios that arise when the nodes interact. This will reveal a certain cyclical evolution of the aggregate behaviour of the nodes, which will lead to the mathematical model that we will develop in Section V.

Whenever a node has a packet to transmit, it starts a random backoff. Once the backoff is completed, the node seeks a reservation of the channel. For that purpose, following the backoff, it performs a CCA, at the start of the next backoff period, to see whether the channel is free. A CCA lasts for 8 symbol times and the CCA status, either success or failure, is revealed at the end of the 8th symbol time. This is because if the channel is declared to be free even at the end of the 8th symbol time, the node can turn its transmitter on within the remaining 12 symbol times and can begin a new transmission at the start boundary of the next backoff period. The actual CCA algorithm involves integrating the observed signal energy over some window, and the result of a CCA is highly dependent on the window, the number of nodes transmitting and their proximity to the node performing the CCA. Hence, in order to facilitate our analysis, we make the simplifying assumption that if any channel activity (successful transmission or collision) finishes before the end of the 8th symbol time in a backoff period, the channel appears to be virtually free from the point of view of all the nodes not involved in the activity. This can be expected to provide a

²Energy saving is an important consideration in sensor networks. In the 802.11 standard nodes keep their receivers on even during backoff periods so that they can sense any transmission and freeze their counters during activity periods. However, carrier sensing also requires energy. In the 802.15.4 standard, during backoff, a node's receiver can shut down and CCA is performed only after backoff is finished, thus saving energy.

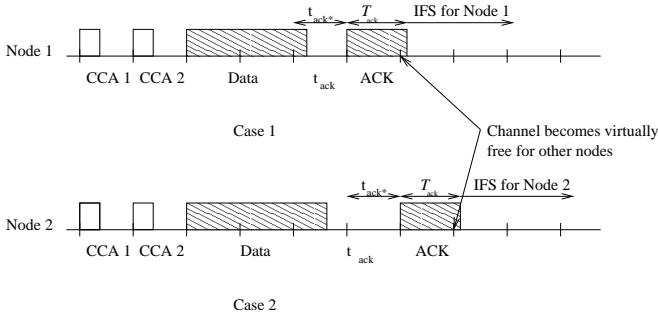


Fig. 4. A successful transmission. If the amount of time occupied by data in its last backoff period is less than 8 symbol times then 12 symbol times remain in the backoff period, sufficient to turn around and send an ACK; then Case 1 occurs. Otherwise the turn around time spills over into the next backoff period and the ACK must start at the beginning of the next backoff period boundary; hence, Case 2 occurs.

higher chance of CCA success, hence leading to optimistic results.

In case the first CCA succeeds, the node waits until the start of the next backoff slot and performs one more CCA. If the channel is again found to be free, the node starts transmission at the start of the next backoff period boundary. The reason for using two CCAs becomes clear from the remaining discussion in this subsection.

A successful transmission is always accompanied by reception of a MAC acknowledgment of length 11 bytes (see Figure 4, where the last byte of the ACK is shown spilling over into the second backoff period). Once a node finishes reception of data, it needs a time t_{ack} (see Figure 3) before its transmitter is turned on, and then it starts transmission of the MAC ACK. Since, transmission of an ACK can start at a backoff period boundary only, t_{ack} can have values in the range: $aTurnaroundTime \leq t_{ack} \leq aTurnaroundTime + aUnitBackoffPeriod$. The whole transaction also includes an interframe space time after transmission of the MAC acknowledgment (see Figure 3).

In case data transmission finishes before the end of the 8th symbol time in its last backoff period, the receiver can turn its transmitter on (during the remaining 12 symbol times) before the start of the next backoff period and, hence, it can start the transmission of the ACK at the next backoff period boundary. But if data requires more than 8 symbol times in its last backoff period, the receiver has less than 12 symbol times in that backoff period and hence the turn around time spills over into the next backoff period. So, the ACK has to wait one more entire backoff period. In either case the channel becomes virtually free for exactly one backoff period. Denote that backoff period by t_{ack^*} . Figure 4 shows these situations.

There will be a collision only if two or more nodes start their first CCA (in the sequence of two CCAs) at the same backoff boundary. A transmitting node always waits for acknowledgment for $macAckWaitDuration$ before declaring a collision. This is the worst case delay which can occur in reception of acknowledgment. Denote the ACK transmission time by \mathcal{T}_{ack} . Then $macAckWaitDuration = \max(t_{ack}) + \mathcal{T}_{ack} = aTurnaroundTime + aUnitBackoffPeriod + \mathcal{T}_{ack}$. This situation

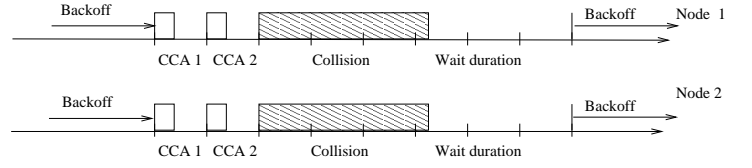


Fig. 5. A collision between two nodes. Both complete their backoffs at the same backoff period boundary, and both CCAs of both nodes find the channel idle. Then the packet transmissions collide.

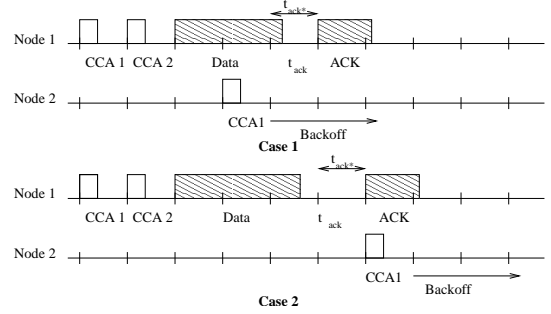


Fig. 6. Node 2 attempts while data or an acknowledgment are being transmitted in Case 1 and Case 2 respectively. In both the cases the channel is not virtually free. Node 2's first CCA fails and it enters its next backoff cycle for the same packet.

is depicted in Figure 5, where nodes 1 and 2 are shown to collide.

While a node performs CCAs, if some activity is going on and the channel is not virtually free, its first CCA itself will fail. This possibility is shown through Figures 6 and 7.

On the other hand, when a node starts a CCA, if the channel is either in second CCA (CCA 2) or in t_{ack^*} due to some node, then the first CCA (CCA 1) from the node will succeed, but this node's CCA 2 will fail. Figures 8 and 9 show the situations where the first CCA succeeds while the second fails for Node 2. This explains why two CCAs are needed.

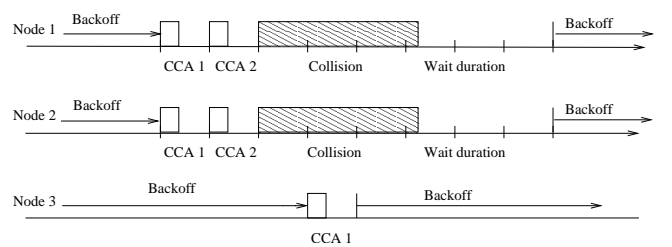


Fig. 7. Node 3 attempts while channel is in collision and not free even virtually. Its first CCA fails and it enters its next backoff cycle for the same packet.

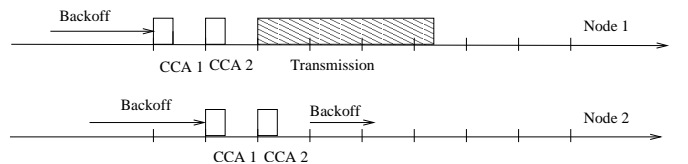


Fig. 8. Node 2 attempts while Node 1 is in a second CCA. Its second CCA fails even when the first has succeeded. Node 1's transmission carries on, while Node 2 enters into the next backoff

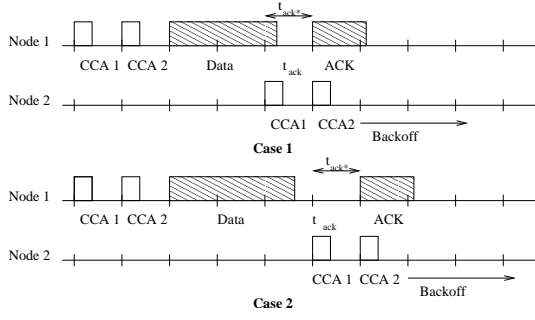


Fig. 9. Node 2 attempts while channel is in t_{ack} . Its second CCA fails even when the first has succeeded. Node 1's transmission carries on, while Node 2 enters into the next backoff

IV. OBSERVATIONS ABOUT THE IEEE 802.15.4 NS2 MODULE

A detailed look at IEEE 802.15.4 ns2 module [14] revealed that there are a few inconsistencies between the module and the IEEE 802.15.4 standard [1]. We made changes in the module to address the following discrepancies, which are relevant to our work.

- 1) A node performing CCA decides whether the CCA has succeeded only at the end of the 8^{th} symbol time in a backoff period. Once the second CCA succeeds, the remaining 12 *symbol times* (which is equal to $aTurnaroundTime$) left in that backoff period are sufficient for the node to turn its transmitter on. In the ns2 module, a node spends one extra backoff period before starting actual transmission, whenever its second CCA succeeds.
- 2) Whenever a node's frame collides, the attempt counter is increased by one until the counter exceeds $aMaxFrameRetries$, after which the frame is discarded. Unlike the standard, in the ns2 module a node resets this counter when the attempt process of a packet spills over into a new superframe.
- 3) In case a channel access failure occurs while attempting for a packet, the packet should be discarded. But in the ns2 module a packet is reattempted indefinitely often after channel access failures, and is discarded only if it faces more than $aMaxFrameRetries$ collisions.

V. THE STOCHASTIC MODEL AND A FIXED POINT EQUATION

A. A Cyclic Evolution

Time is divided into contiguous backoff periods whose duration is denoted by δ . All node activities are initiated at backoff period boundaries. We need to study each node's individual behavior and also the aggregate channel activity. From the point of view of the channel activity, we can define certain cycles (see the last time line in Figure 10). There could be a succession of idle backoff periods. An idle channel period ends when both of the successive CCAs of one or more nodes are successful. Once this happens, the channel activity in the following cycle can evolve in one of two ways: i.e., subsequently there may be a successful transmission (as in

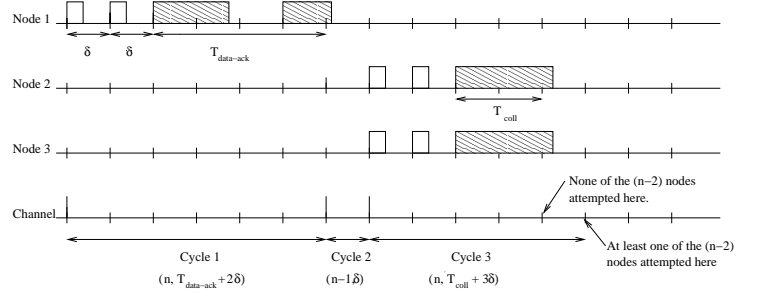


Fig. 10. A snapshot of evolution of the activity at three nodes. The fourth time-line superposes these activities, thus depicting a cyclical evolution for the aggregate system.

case of Node 1 in Figure 10), or a collision between two or more nodes (like Nodes 2 and 3 in Figure 10).

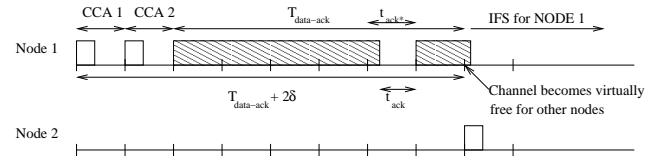


Fig. 11. A successful transmission. It lasts for $T_{data-ack} + 2\delta$ duration, the channel is virtually free at the time shown and only $n - 1$ nodes are available for attempt in the following backoff period.

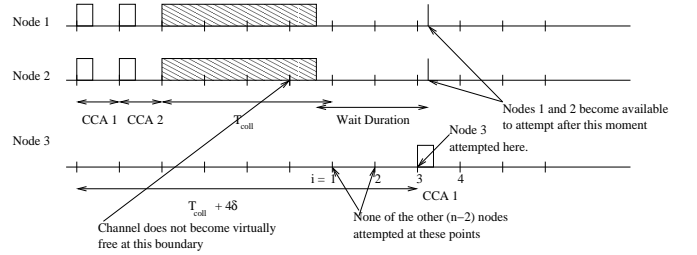


Fig. 12. A cycle containing collisions. Its length is $T_{coll} + 4\delta$ because Node 3 has attempted at the 3^{rd} backoff period boundary after collision is over. Only $n - 2$ nodes were available there to attempt at that point for new cycle.

Suppose the network consist of n contending nodes, excluding the PAN coordinator. The length of a cycle depends on the *number of nodes available to attempt* in the first backoff period of the cycle. A cycle contains a single idle backoff period of length δ , if none of the available nodes attempts to sense the channel at the start boundary of this backoff period (see Cycle 2 in Figure 10). It leaves all those nodes free to attempt in the next cycle.

In Figure 11 we show a successful transmission cycle. Let us examine this carefully. The total busy period of the transaction is shown as $T_{data-ack}$. Acknowledgments always start at the boundary of a backoff period and being of fixed length 11 bytes (i.e., 22 symbols) consume only 2 symbol times in their last backoff period. Thus, at the start boundary of this backoff period, the channel becomes *virtually free* for other nodes because a CCA that starts at this backoff period boundary (being of 8 symbol times duration) will find the channel clear, and hence a new cycle might be started by other nodes in

this backoff period. Thus, $T_{data-ack}$ does not include this backoff period. Define $T_{data-ack}^*$ as the portion of $T_{data-ack}$, excluding t_{ack}^* (recalling t_{ack}^* from Section III) i.e.,

$$T_{data-ack}^* = T_{data-ack} - t_{ack}^*$$

It is seen that, a cycle of successful transmission lasts for $T_{data-ack} + 2\delta$ duration and, only $n-1$ nodes are available for attempt in the following backoff period. Note from Figure 10 that the channel is viewed as being in an idle cycle (Cycle 2) even though the transmission of Node 1 is not complete.

In Figure 12 we depict a collision cycle. If there are 2 or more nodes available to attempt at the beginning of a cycle, there is a possibility of collision. If there is a collision of k nodes, it continues for T_{coll} duration. During its last backoff period, if a collision consumes less than or equal to 8 symbol times, again the channel becomes virtually free from the point of view of nodes not involved in collision; then, this backoff period is not included in T_{coll} . After the collision, all the k senders wait for acknowledgment for $macAckWaitDuration$ before realising that there is a *transmission failure*. Define a positive integer J such that

$$J + 1 = \left\lceil \frac{T_{coll} + macAckWaitDuration}{\delta} \right\rceil + 2 - \frac{T_{coll}}{\delta}$$

where T_{coll} is the actual time spent in collision by a node. A careful look at various parameters reveals that the only possible values of J are 4 and 5. Thus a cycle containing a collision activity has one of the following three possibilities.

- Case 1: $k < n$, and one or more of the $n - k$ nodes not involved in the collision perform successful CCAs, while k nodes involved in collision are still waiting for acknowledgments. In this case the length of the current cycle will be $T_{coll} + j\delta$, $j \in \{2, 3, \dots, J\}$ with, $n - k$ nodes being available to contend for next cycle. Also the next cycle cannot be an idle cycle.
- Case 2: $k < n$, and all the k nodes involved in the collision finish with their $macAckWaitDurations$ and none of the other $n - k$ nodes attempts for a CCA in this duration. In this case the length of the current cycle will be $T_{coll} + (J + 1)\delta$, and all the n nodes will be available to contend for next cycle.
- Case 3: $k = n$. There will not be any node available to attempt after the collision is over. The current cycle will last for $T_{coll} + (J + 1)\delta$ duration, and all the n nodes will be available to contend for next cycle.

These situations are illustrated by Figure 12, which corresponds to $J = 4$. Here the current cycle may be of lengths $T_{coll} + (i + 1)\delta$, $i = 1, 2, 3$, provided that some of the nodes other than 1 or 2, attempt at the i^{th} backoff period boundary after the collision is over. The cycle length will be $T_{coll} + 5\delta$ if none of other nodes attempt while nodes 1 and 2 are waiting for acknowledgments. The figure shows the case where the cycle length is $T_{coll} + 4\delta$. In Figure 10 the channel enters into Cycle 4, while Nodes 2 and 3 are still waiting for acknowledgments.

B. The Stochastic Model

As shown in Section V-A, the cycles defined are always multiples of the backoff period. Denote the backoff period boundaries by $t_k = k\delta$, $k \geq 0$. Then denote the start times of the cycles by the random times T_i , $i \geq 0$, with $T_i \in \{t_j : j \geq 0\}$, and $T_0 (= 0) < T_1 < T_2 < \dots$. Associated with each T_i , $i \geq 0$, is a random variable $X_i \in \{1, 2, \dots, n\}$, which is the number of nodes available to attempt at the instant T_i . The cycles are indexed by $i \geq 1$, with cycle i being the interval $[T_{i-1}, T_i)$. Denote the cycle length by

$$U_i = T_i - T_{i-1}$$

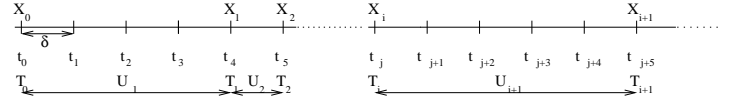


Fig. 13. Channel cycles and notation for the Markov renewal process

We draw the following conclusions from the discussion of Section V-A.

- If $X_i = n$, then Cycle $i + 1$ may comprise a successful transmission, a collision, or the cycle may be an idle one, depending upon the number of nodes that attempt.
- If $X_i = n - 1$ (as would happen after a success cycle), then Cycle $i + 1$ may have a successful transmission, a collision, or the cycle may be an idle one, depending upon the number of nodes that attempt.
- If $X_i < n - 1$, it means we are in a case like that shown in Figure 12, i.e., at least one of these nodes has attempted, and the following cycle cannot be an idle one. It can have a successful transmission or a collision depending upon how many nodes have attempted.

It is seen that, if the number of nodes available to attempt at the beginning of the cycle is known, the evolution of the cycles in the future does not depend on the past, i.e., the random vector (U_{i+1}, X_{i+1}) and the random vector $((X_0, T_0), (X_1, T_1), \dots, (X_{i-1}, T_{i-1}), T_i)$ are independent, given X_i . Hence, although the cycles are not independent, (X_i, T_i) , $i = 0, 1, 2, \dots$ is a Markov renewal process. To analyse this we need the transition probabilities

$$P(U_{i+1} = u, X_{i+1} = k' | X_i = k')$$

for all possible values of u , k and k' . Also, $\{X_i, i \geq 0\}$ will be a Markov chain. We can obtain the transition probability matrix \mathbf{M} for this Markov chain, and hence we can compute the steady state probabilities π_k , $1 \leq k \leq n$.

Given the number of nodes available to attempt at the beginning of a cycle, the conditional expectation of the corresponding cycle length can be developed, and we can define the following quantities. For $1 \leq k \leq n$ (and any i) define,

$$E_k U = \sum_u u \sum_{k'} P(U_{i+1} = u, X_{i+1} = k' | X_i = k)$$

Then, the expected duration of a cycle will be given as

$$EU = \sum_{k=1}^n \pi_k E_k U$$

$r^{(e)}(u, k)$		e					
		CCA2	$T_{data-ack}$	T_{coll}	$T_{data-ack}^*$	t_{ack}^*	successfully sent data
(u, k)	(δ, n)	0	0	0	0	0	0
	$(T_{data-ack} + 2\delta, n - 1)$	δ	$T_{data-ack}$	0	$T_{data-ack} - \delta$	δ	L_{data}
	$(T_{coll} + j\delta, k)$ $j \in \{2, 3, \dots, J\}$ $k \in \{1, 2, \dots, (n-2)\}$	δ	0	T_{coll}	0	0	0
	$(T_{coll} + (J+1)\delta, n)$	δ	0	T_{coll}	0	0	0

TABLE I

VALUES OF $r^{(e)}(u, k)$ FOR SEVERAL e S AND ALL POSSIBLE (u, k) S. IT CAN BE SEEN THAT $R_i^{(e)}$ CAN BE UNIQUELY DETERMINED, GIVEN (U_i, X_i) .

We can also determine the conditional expected durations for which channel is either in second CCA, $T_{data-ack}$ or T_{coll} , in a cycle. More generally, suppose, in the i^{th} cycle the channel remains in event e for an amount of time $R_i^{(e)}$. Thus, $R_i^{(e)}$ can be considered as a ‘‘reward’’ (corresponding to the occurrence of event e) in the i^{th} cycle. It can also be shown that, for each event e of interest, $R_i^{(e)}$ will be a *function* of (U_i, X_i) (see Table I). By this we mean that for each event of interest e , there is a function $r^{(e)}(u, k')$, such that, for all possible values of u, k' and any i , if $(U_i, X_i) = (u, k')$ then $R_i^{(e)} = r^{(e)}(u, k')$. Note that $\{R_i^{(e)}, i \geq 1\}$ are such that, given $X_i, R_{i+1}^{(e)}$ and $((X_0, T_0), (X_1, T_1), \dots, (X_{i-1}, T_{i-1}), T_i)$ are independent. Then we define (for any i)

$$E_k R^{(e)} = \sum_u \sum_{k'} r^{(e)}(u, k') P(U_{i+1} = u, X_{i+1} = k' | X_i = k)$$

Now, the expected duration for which the channel remains in event e in a cycle, can be obtained as

$$E(R^{(e)}) = \sum_{k=1}^n \pi_k E_k R^{(e)}$$

Let $R^{(e)}(t)$ be the duration during $[0, t]$ for which the channel is in event e . Then by a regenerative argument (or the Markov renewal reward theorem) we see that, with probability 1,

$$\lim_{t \rightarrow \infty} \frac{R^{(e)}(t)}{t} = \frac{\sum_{k=1}^n \pi_k E_k R^{(e)}}{\sum_{k=1}^n \pi_k E_k U}$$

Hence various event rates in the system can be determined (e.g., the throughput of good packets can be obtained this way).

C. A Decoupling Approximation

Motivated by the approach in [4] and [10], we propose a decoupling approximation in order to analyse the above process. In this section we provide an outline of our approach. Each node alternates between periods when it performs backoffs and unsuccessful CCAs and periods when it transmits (successfully or unsuccessfully). Let β denote the rate at which a node’s backoffs complete during the time when it is performing backoffs; i.e., β is a rate conditioned on times during which the node is performing back-offs. Unlike the IEEE 802.11 DCF mechanism, here nodes do not freeze their backoff timers when there is activity on the channel. So, it is not possible to work with ‘‘conditional time’’ as is done in [10] to facilitate the fixed point analysis for 802.11 WLANs. Instead we proceed

as follows. As shown in Figure 10, the channel evolves over cycles. At the end of each cycle we need to determine the activity in the next cycle. The nodes that can attempt in the next cycle are in their backoff periods. We assume that each such node attempts independently in a slot with probability β . Thus, if k nodes can potentially attempt at a backoff period boundary, then we assume that the number of attempts is binomially distributed with parameters k and β . With this assumption, the transitions probabilities of the Markov renewal process, and the conditional expectations defined in Section V-B can be written down. The detailed derivation of the transitions probabilities and conditional distributions are provided in the Appendix. This approach permits us to obtain channel event rates in terms of the unknown value β .

In order to obtain β , we separate out a typical (‘‘tagged’’) node and analyse it while viewing the other nodes as an *environment*. We can express β in terms of certain channel activity measures of other nodes. It is shown in Section V-D that there is a function $G(\cdot, \cdot, \cdot)$ such that

$$\beta = G(\alpha, \alpha_{data-ack}^*, \alpha_{coll})$$

where α is the probability that the tagged node’s CCA fails, $\alpha_{data-ack}^*$ is the probability that the tagged node finds one of the other nodes in a successful transmission, and α_{coll} is the probability that the tagged node finds some of the other nodes in a collision. In the overall analysis procedure, we can call the above equation a typical node’s *response equation*, with the various probabilities capturing the *influence* of the environment on the tagged node. Each of these probabilities are obtained as a certain fraction of time that the other $n - 1$ nodes (i.e., the environment in relation to the tagged node) are in certain states. For example, α_{coll} is the fraction of time that the other $n - 1$ nodes are in a collision. In order to obtain these probabilities we proceed as follows: (i) It is assumed that each node in the environment also behaves like the tagged node, and hence attempts during its back-off periods at the rate β , and (ii) then we obtain the desired fractions of times by assuming that when several nodes are performing back-offs they attempt *independently*, each with probability β . This latter approximation is exactly the kind of approximation in other fixed point based analyses such as in [4] and [10]. This yields equations that can be called the *coupling equations*.

In order to obtain the coupling equations, we obtain the probabilities of various events occurring when each of the $n - 1$ nodes (that comprise the tagged node’s environment) uses the (unknown) attempt rate β . The channel evolves over cycles as

shown in Figure 10. Using the Markov regenerative analysis described in Section V-B we find the fraction of time occupied by certain events (e.g., a collision). As per the decoupling approximation, we assume that the tagged node see the events with this probability. Thus channel activity measures seen by the tagged node can be determined in terms of β , e.g., $\alpha = H(n-1, \beta)$, $\alpha_{coll} = H_{coll}(n-1, \beta)$, etc., where the $H_{\dots}(\cdot, \cdot)$ functions are shown in Section V-D. This yields β in terms of the activity measures of the environment, and vice versa. This gives the following fixed point equation.

$$\beta = G(H(n-1, \beta), H_{data-ack^*}(n-1, \beta), H_{coll}(n-1, \beta))$$

The fixed point equation yields β , which can then be used to obtain the aggregate saturation throughput of the network. The details are developed in Section V-D.

D. A Fixed Point Equation for β

Let us tag a node and obtain its β . A CCA from the tagged node will fail if it finds the channel either in second CCA, $T_{data-ack}$ (see Figure 11) or T_{coll} (see Figure 12). Let α_{CCA2} , $\alpha_{data-ack}$ and α_{coll} be the probabilities of the channel being in second CCA, $T_{data-ack}$ or T_{coll} respectively. Then considering each of these as an event e , we can use the analysis in Section V-B to obtain their time rates. Noting that once we have tagged a node we need to find the above probabilities for the other $n-1$ nodes, the desired probabilities are given as:

$$\begin{aligned} \alpha_{CCA2} &= \frac{\sum_{k=1}^{n-1} \pi_k E_k R^{(CCA2)}}{\sum_{k=1}^{n-1} \pi_k E_k U} =: H_{CCA2}(n-1, \beta) \\ \alpha_{data-ack} &= \frac{\sum_{k=1}^{n-1} \pi_k E_k R^{(data-ack)}}{\sum_{k=1}^{n-1} \pi_k E_k U} =: H_{data-ack}(n-1, \beta) \\ \alpha_{coll} &= \frac{\sum_{k=1}^{n-1} \pi_k E_k R^{(coll)}}{\sum_{k=1}^{n-1} \pi_k E_k U} =: H_{coll}(n-1, \beta) \end{aligned}$$

Note that the right hand sides of the above three equations depend on β . Hence α , the probability that a tagged node's CCA will fail, can be given in terms of β as

$$\alpha = H(n-1, \beta)$$

where $H(n-1, \beta) := \alpha_{CCA2} + \alpha_{data-ack} + \alpha_{coll}$, with each term being given as above. Also let $\alpha_{data-ack^*}$ and $\alpha_{t_{ack^*}}$ be the fractions of time, the channel is in $T_{data-ack^*}$ and t_{ack^*} respectively. These quantities can also be calculated as functions of β , in the way shown above. Let

$$\begin{aligned} \alpha_{data-ack^*} &= \frac{\sum_{k=1}^{n-1} \pi_k E_k R^{(data-ack^*)}}{\sum_{k=1}^{n-1} \pi_k E_k U} \\ &:= H_{data-ack^*}(n-1, \beta) \\ \alpha_{t_{ack^*}} &= \frac{\sum_{k=1}^{n-1} \pi_k E_k R^{(t_{ack^*})}}{\sum_{k=1}^{n-1} \pi_k E_k U} := H_{t_{ack^*}}(n-1, \beta) \end{aligned}$$

Evidently, $\alpha_{data-ack} = \alpha_{data-ack^*} + \alpha_{t_{ack^*}}$.

Having obtained these channel probabilities in terms of β , we now turn to obtaining β in terms of the channel probabilities, thus leading to a fixed point equation. Recall that all the

nodes have saturated queues. A node goes through the backoff procedure for its head-of-the-line (HOL) packet. Each such backoff procedure can end in one of three ways: successful transmission, collision, or a channel access failure (i.e., none of the CCAs during the backoff procedure succeeds). If there is a success, a fresh backoff procedure is begun for the next packet. If there is a collision, a fresh backoff procedure is begun for the same packet and the packet is discarded after N collisions ($N = 4$ in the standard, as 3 retries are allowed). Upon the discard of a packet a fresh backoff procedure is begun for the next packet. Finally, if there is a channel access failure for a packet, the packet is discarded, and the next packet moves to the HOL position. We seek β , the rate at which backoffs complete during times when the tagged node is performing backoffs, given the various probabilities for the other $n-1$ nodes, as obtained above. Let us denote

- K = the number of times channel sensing is reattempted in a backoff cycle
- b_k = the mean backoff duration (in backoff periods) before the $(k+1)^{th}$ channel sensing attempt for a packet, $0 \leq k \leq K$

It must be noted that during a backoff procedure, each backoff will be followed by one or possibly two CCA durations before the next backoff starts following a CCA failure.

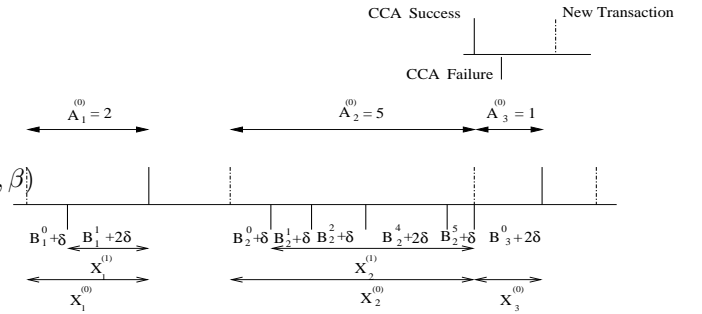


Fig. 14. Evolution of backoff, channel sensing and busy periods for a tagged node. The first backoff procedure had two CCAs, the second of which succeeded (see legend on top right). The procedure took an amount of time $X_1^{(0)}$. The second backoff procedure had 5 CCAs and ended in failure. The third had one CCA which was successful. Note that a successful CCA could result in a collision. Then the backoff rate during backoff times, over this fragment of the node's evolution is $\frac{2+5+1}{X_1^{(0)} + X_2^{(0)} + X_3^{(0)}}$.

Suppose, $A_j^{(k)}$ denotes the number of attempts for the j^{th} backoff procedure after the k^{th} backoff failure. Thus, $A_j^{(0)}$ will give the total number of attempts for the backoff procedure and the sequence of backoff times will be $B_j^{(k)}$ ($0 \leq k \leq A_j^{(0)} - 1$), with $E(B_j^{(k)}) = b_k$. Also let $X_j^{(k)}$ be the time duration for j^{th} backoff procedure between the k^{th} backoff failure and the end of the backoff procedure. Then $X_j^{(0)}$ will denote the total time occupied by the j^{th} backoff procedure. Evolution of the backoff, channel sensing and busy periods for a node are shown in Figure 14.

Under the decoupling approximation we observe that the sequence $X_j^{(0)}$, $j \geq 1$, are renewal life times. Viewing the total number of attempts in the j^{th} backoff procedure, $A_j^{(0)}$, as a

“reward” associated with the renewal cycle of length $X_j^{(0)}$, we see from the renewal reward theorem that the attempt rate β of a node during its backoff period is given by $\frac{E(A_j^{(0)})}{E(X_j^{(0)})}$. We now derive expression for this ratio in terms of the channel probabilities obtained earlier.

We assume that the CCAs of the tagged node “see” the remaining $n - 1$ nodes in equilibrium and hence that the probability that the tagged node’s CCA fails is α . Thus

$$E(A_j^{(0)}) = 1 + \alpha E(A_j^{(1)})$$

and, further

$$E(A_j^{(1)}) = 1 + \alpha E(A_j^{(2)})$$

Hence recursing (using $E(A_j^{(K)}) = 1$) we get

$$E(A_j^{(0)}) = \sum_{k=0}^K \alpha^k$$

We now turn to $E(X_j^{(0)})$. A node’s first CCA will fail if it finds the channel in $T_{data-ack^*}$ or T_{coll} . Its first CCA will succeed while the second will fail if the channel is in the second CCA or t_{ack^*} . Hence,

$$\begin{aligned} E(X_j^{(0)}) &= b_0 + (\alpha_{data-ack^*} + \alpha_{coll})(\delta + E(X_j^{(1)})) \\ &\quad + (\alpha_{CCA2} + \alpha_{t_{ack^*}})(2\delta + E(X_j^{(1)})) + (1 - \alpha)2\delta \end{aligned}$$

Using the fact that

$$\alpha = \alpha_{data-ack^*} + \alpha_{t_{ack^*}} + \alpha_{coll} + \alpha_{CCA2}$$

we get

$$E(X_j^{(0)}) = b_0 + \alpha E(X_j^{(1)}) + (2 - (\alpha_{data-ack^*} + \alpha_{coll}))\delta$$

Similarly

$$E(X_j^{(1)}) = b_1 + \alpha E(X_j^{(2)}) + (2 - (\alpha_{data-ack^*} + \alpha_{coll}))\delta$$

Again recursing, with $E(X_j^{(K)}) = b_K + (\alpha_{data-ack^*} + \alpha_{coll})\delta + (\alpha_{CCA2} + \alpha_{t_{ack^*}})2\delta + (1 - \alpha)2\delta$, we get

$$E(X_j^{(0)}) = \sum_{k=0}^K \alpha^k (b_k + (2 - (\alpha_{data-ack^*} + \alpha_{coll}))\delta)$$

Thus, the attempt rate β can be obtained as

$$\begin{aligned} \beta &= \frac{\sum_{k=0}^K \alpha^k}{\sum_{k=0}^K \alpha^k (b_k + (2 - (\alpha_{data-ack^*} + \alpha_{coll}))\delta)} \\ &:= G(\alpha, \alpha_{data-ack^*}, \alpha_{coll}) \end{aligned}$$

Now, it can be expected that the equilibrium behavior of the system will be characterized by the solutions of the following fixed point equation:

$$\begin{aligned} \beta &= G(H(n-1, \beta), H_{data-ack^*}(n-1, \beta), H_{coll}(n-1, \beta)) \\ &=: \Gamma(\beta) \end{aligned}$$

Since $G(\cdot)$, $H(\cdot)$, $H_{data-ack^*}(\cdot)$ and $H_{coll}(\cdot)$ are continuous functions so is $\Gamma(\cdot)$. Thus $\Gamma(\cdot)$ is a continuous map from $[0, 1]$ to $[0, 1]$ and hence by Brouwer’s fixed point theorem there is a fixed point.

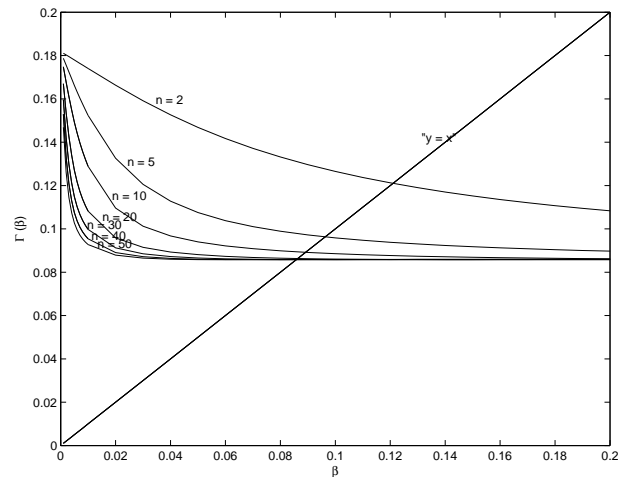


Fig. 15. $\Gamma(\beta)$ vs β for several values of n . The intersections with the “ $y = x$ ” line yield the fixed points.

Numerical solution of the fixed point equation. We assume operation in the 2.45GHz band and hence the PHY data rate is 250 Kbps. The backoff multiplier is $p = 2$ as in the IEEE 802.15.4 standard. In the plots we use the following values: $K = 4$, $macMinBE = 3$, $aMaxBE = 5$, and $b_0 = 3.5$ backoff periods. The packet size (MSDU) is assumed to be 30 bytes throughout. Figure 15 shows plots of $G(H(n-1, \beta), H_{data-ack^*}(n-1, \beta), H_{coll}(n-1, \beta))$ vs. β . The intersections of the plots with the “ $y = x$ ” line yield the fixed points. We obtain the fixed points by using the `fzero()` function in MATLAB. At this point in our work we are unable to analytically show uniqueness. However, in all the cases we examined the fixed point was unique. We see that for this set of parameters the attempt rate of the individual nodes remains almost constant (at about 0.086) once the number of nodes exceeds 10.

VI. CALCULATION OF PERFORMANCE MEASURES

A. Throughput Calculation

To calculate the throughput, we again use the Markov renewal process formulated earlier in Section V-B. Successfully sent data in a cycle can be considered as yet another “reward” associated with that cycle.

A successful data transmission will take place in cycle i only if $(U_i, X_i) = (T_{data-ack} + 2\delta, n-1)$. Consider L_{data} as the size of a packet. Then the expected amount of data sent in a cycle, having k nodes to attempt at its beginning, is given by:

$$E_k L = L_{data} P(U_{i+1} = T_{data-ack} + 2\delta, X_{i+1} = n-1 | X_i = k)$$

Note that once we have β from the fixed point approach we analyse the entire system of n nodes; hence, the summations in this section will run up to n . Hence the expected amount of data sent in a cycle, will be given by

$$E(L) = \sum_{k=1}^n \pi_k E_k L$$

Now, using the renewal reward theorem, the aggregate throughput of the system with n sensor nodes can be seen to be:

$$\Theta(n) = \frac{\sum_{k=1}^n \pi_k E_k L}{\sum_{k=1}^n \pi_k E_k U}$$

Throughput calculation for a network with a single sensor: For the case of a single node, a much simpler analysis gives the saturation throughput. The average time required for transmission of a packet will be $b_0 + 2\delta + \delta \lceil \frac{\mathcal{T}_{data-ack}}{\delta} \rceil$, where $\mathcal{T}_{data-ack}$ is actual time required for transmission of data and the corresponding acknowledgment, including t_{ack} . Since a new transaction can start at next backoff period boundary only, $\frac{\mathcal{T}_{data-ack}}{\delta}$ has been rounded up. Then,

$$\Theta(1) = \frac{L_{data}}{b_0 + 2\delta + \lceil \frac{\mathcal{T}_{data-ack}}{\delta} \rceil \delta}$$

For a payload of 10 bytes, $L_{data} = 30$ bytes. Taking into account all headers, t_{ack} and acknowledgment, $\mathcal{T}_{data-ack} = 122$ symbol times (6.1 backoff periods). Hence $\lceil \mathcal{T}_{data-ack} \rceil = 7$ backoff periods. With the backoff parameters in the standard, $b_0 = 3.5$ backoff periods. Hence $\Theta(1) = 30$ bytes /12.5 backoff periods = 60 kbps or 250 packets per second.

B. Packet Discard Analysis

It is known from the description of the slotted CSMA/CA algorithm that the backoff cycle for a frame may end with either a successful transmission, a collision or a channel access failure. In case a backoff failure occurs, the frame is discarded without any reattempt. If a frame collides, it is retried $aMaxFrameRetries$ times. A frame will collide only if while attempting for this frame, the node finds the channel in first CCA. Let α_{CCA1} be the probability of the channel being in first CCA. Then, using the approach in Section V-B, the probability that a frame collides, given that it is attempted, can be written as:

$$\alpha_{CCA1} = \frac{\sum_{k=1}^n \pi_k E_k R^{(CCA1)}}{\sum_{k=1}^n \pi_k E_k U} =: H_{CCA1}(n, \beta)$$

Let $p_{i,j}$ be the probability of a packet being successfully served after it has faced i collisions and is in the j^{th} backoff of current backoff cycle ($0 \leq j \leq K$). Then $p_{0,0}$ will be the probability that a packet is successfully served. We recall that K and N denote $macMaxCSMABackoffs$ and $aMaxFrameRetries$ respectively. We see that

$$p_{0,0} = 1 - (\alpha + \alpha_{CCA1}) + \alpha_{CCA1} p_{1,0} + \alpha p_{0,1}$$

and, also

$$p_{0,1} = 1 - (\alpha + \alpha_{CCA1}) + \alpha_{CCA1} p_{1,0} + \alpha p_{0,2}$$

Recurring (using $p_{0,K} = 1 - (\alpha + \alpha_{CCA1}) + \alpha_{CCA1} p_{1,0}$), we

get

$$\begin{aligned} p_{0,0} &= \sum_{k=0}^K \alpha^k (1 - (\alpha + \alpha_{CCA1}) + \alpha_{CCA1} p_{1,0}) \\ &= \frac{(1 - (\alpha + \alpha_{CCA1}))(1 - \alpha^{K+1})}{1 - \alpha} \\ &\quad + \frac{\alpha_{CCA1}(1 - \alpha^{K+1})}{1 - \alpha} p_{1,0} \end{aligned}$$

Similarly

$$\begin{aligned} p_{1,0} &= \frac{(1 - (\alpha + \alpha_{CCA1}))(1 - \alpha^{K+1})}{1 - \alpha} \\ &\quad + \frac{\alpha_{CCA1}(1 - \alpha^{K+1})}{1 - \alpha} p_{2,0} \end{aligned}$$

Again recurring (with $p_{N+1,0} = 0$), we get

$$\begin{aligned} p_{0,0} &= \sum_{k=0}^N \left(\frac{\alpha_{CCA1}(1 - \alpha^{K+1})}{1 - \alpha} \right)^k \\ &\quad \left(\frac{(1 - (\alpha + \alpha_{CCA1}))(1 - \alpha^{K+1})}{1 - \alpha} \right) \end{aligned}$$

Then, the probability of a packet being discarded will be given by

$$P_{discard} = 1 - p_{0,0}$$

Define $D(n)$ to be the rate of discarded packets with n saturated nodes. By definition

$$P_{discard} = \frac{D(n)}{\Theta(n) + D(n)}$$

Hence

$$D(n) = \frac{\Theta(n)}{1 - P_{discard}} P_{discard}$$

VII. NUMERICAL RESULTS AND SOME INSIGHTS

For the simulation results ns2 version 2.26 is used, with patches for the IEEE 802.15.4 LR-WPAN code provided by J. Zheng[14]. We have used the source code released on January 1, 2005, with modifications as discussed in Section IV. Static routing is implemented by using NOAH as the wireless routing agent. This allows us to ensure multihop wireless routing is not used. We work in the 2.45 GHz band, with the PHY data rate 250 Kbps. The simulation scenario consists of n nodes distributed uniformly around a circle of radius 8 meters, with the PAN coordinator at the center. The decoding and the sensing range thresholds of the nodes are set to 20 meters, so that all nodes form a single cell. Nodes start associating with the PAN coordinator one by one at regular intervals of 0.5 seconds. After 5.0 seconds of the last node having started association, CBR traffic is initiated simultaneously from all the nodes. The CBR packet size is kept as 10 bytes to which 20 bytes of IP header, 7 bytes of MAC header and 6 bytes of PHY header are added. To ensure saturation, the CBR traffic interval is kept very small; each node's buffer receives packets at intervals of 5 ms. Where the throughput results are in bytes/sec, and represent the throughput of the MAC payload.

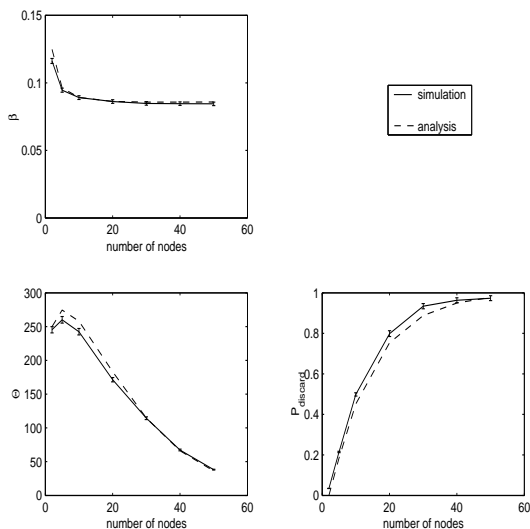


Fig. 16. Analytical and ns2 simulation results for β , $\Theta(n)$ (packets per second), and $P_{discard}$ vs. n . Simulation results are accompanied by 95% confidence intervals.

A. Results and Observations

The conditional attempt rates per node, β , aggregate throughputs, Θ (packets per second), and discard probabilities, $P_{discard}$, obtained through simulation are compared against the analytical results in Figure 16, where 95% confidence intervals are also shown for the simulation results. We make the following observations:

- It can be seen that, even after many modeling simplifications, the fixed point analysis provides an excellent approximation, for a wide range of the number of nodes, n .
- The results show that β decreases until $n = 10$ and then remains almost constant with increasing n , while the aggregate throughput increases initially but then decreases very sharply with increasing n . The slight increase in Θ with n is because for small n the contention is less and increasing n increases the channel utilisation.
- The discard probability increases rapidly as the number of nodes increases and approaches approximately 1 as the number of nodes is increased up to 50.

We will see later that finite load performance is substantially better, and, in fact, derivable from the saturation performance.

B. Discussion of Default Backoff Parameters

If the expression for $\Theta(\cdot)$ in Section VI-A is evaluated with β as a free variable, for various values of β and n , then we obtain the plots in Figure 17; note that here Θ is given in Kbps (60 Kbps = 250 packets per second). For $n \geq 10$, the values of β for which the aggregate throughput Θ peaks are much less than those obtained for the actual system for the default parameters (about 0.09; see Figure 16). Figure 17 also shows that once a node exceeds these attempt rates its throughput starts decreasing as the attempt rate increases. This is the region, in which the network operates with the current set of backoff parameters ($\beta = 0.09$, see Figure 16). Figure 17

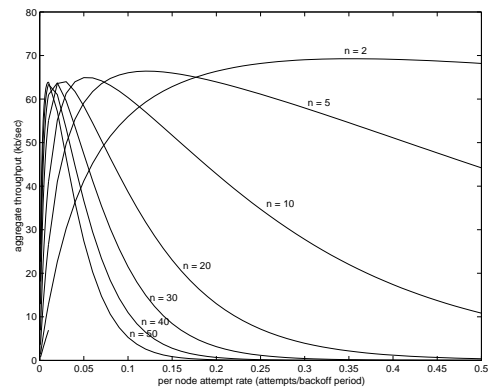


Fig. 17. Aggregate throughput (Θ in Kbps) plots for various n as a function of β , obtained from the stochastic analysis.

shows that in this regime of operation, to maintain a constant throughput as n increases, β must decrease sharply with n ; this does not occur with the given backoff parameters.

It is also observed from Figure 17 that the same throughputs can be obtained with much smaller attempt rates, while working in a region where throughput increases with attempt rate for a fixed number of nodes. The attempt rates, collision probabilities and hence energy expenditure is much less in this region. This also leads to lower discard probabilities. It is also seen that the attempt rate need not decrease significantly in this region to maintain a constant throughput with increasing number of nodes.

C. Performance with Alternate Backoff Parameters

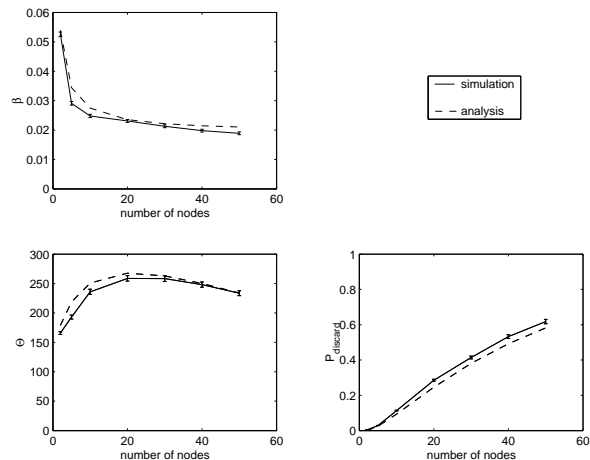


Fig. 18. Analytical and ns2 simulation results for various parameters vs. number of nodes. Plots have been obtained using backoff multiplier $p = 3$. Simulation results show 95% confidence intervals.

We find that simple changes in the backoff parameters can lead us to operate in the desired region. Figures 18 and 19 show the results for two ways of altering the backoff parameters: (i) increasing the backoff multiplier to 3, and (ii) changing macMinBE to 5 and aMaxBE to 7. Figure 18 shows the attempt rate, throughput and discard probability plots after we have increased the backoff multiplier from 2 to 3. Figure 19

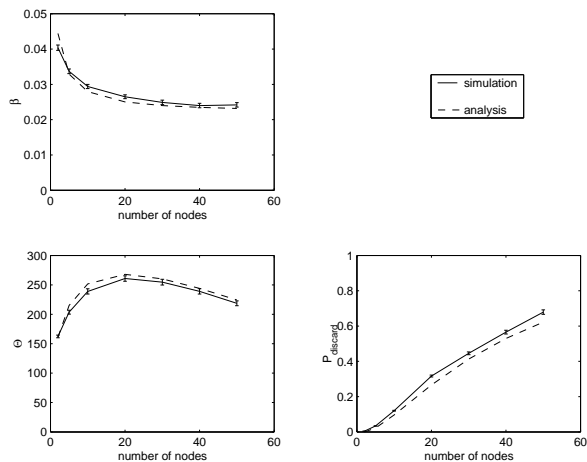


Fig. 19. Analytical and ns2 simulation results for various parameters vs number of nodes. Plots have been obtained with $macMinBE = 5$ and $aMaxBE = 7$. Simulation results show 95% confidence intervals.

is for the case when $macMinBE$ and $aMaxBE$ have been changed to 5 and 7 respectively. These plots show that, with a slight change of a few backoff parameters we are able to maintain constant throughput with increasing number of nodes. Discard probabilities are also substantially smaller. The large initial backoffs cause less contention in the case of a large number of nodes, but on the other hand lead to unnecessary wastage of channel time when number of nodes is small. Hence, we get worse throughputs as compared to those with default parameters for small number of nodes (see Figures 18 and 19). Thus it becomes interesting to consider the possibility of adapting the backoff parameters depending on the number of nodes n , in an attempt to achieve an attempt rate that yields the peak saturation throughput for each n (see Figure 17).

VIII. ANALYSIS WITH FINITE ARRIVAL RATES

Each sensor node receives (generates) packets that have to be delivered to the hub node. We assume that the rate of “arrival” of packets at each sensor node is λ and the arrival processes are independent and Poisson. Note that while a Poisson arrival model would not be appropriate in a regular wireless network that handles packet voice or TCP controlled data, here in a sensor networking context the arrivals are “open loop,” and a Poisson process may be a reasonable model for the occurrence of asynchronous events. Define $\Lambda = n\lambda$.

Let ρ denote the fraction of time a sensor node’s queue is nonempty and hence the node is contending for the channel. As before, $\Theta(n)$ and $D(n)$ are the aggregate throughputs and discard rates for a network with n saturated nodes. We adopt an approach suggested in [8, Chapter 4]. For fixed n , define

$$\mu(n, \rho) = \sum_{m=1}^n \binom{n}{m} \rho^m (1-\rho)^{n-m} (\Theta(m) + D(m))$$

and,

$$\nu(n, \rho) = \sum_{m=1}^n \binom{n}{m} \rho^m (1-\rho)^{n-m} \Theta(m)$$

Thus, given ρ , $\mu(\rho)$ is an approximation for the rate at which packets are being removed from the queue, either by successful transmission or discard. Similarly, $\nu(\rho)$ is an approximation for the rate of successful transmission. It can be seen that $\lim_{\rho \rightarrow 1} \mu(n, \rho) = \Theta(n) + D(n)$, and $\lim_{\rho \rightarrow 1} \nu(n, \rho) = \Theta(n)$. Figure 20 shows plots of $\mu(\rho)$ vs. ρ and $\nu(\rho)$ vs. ρ for several

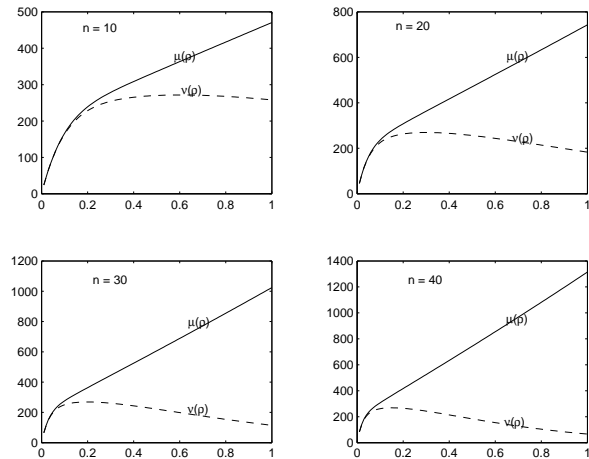


Fig. 20. $\mu(\rho)$ (pkts/sec) and $\nu(\rho)$ (pkts/sec) vs. ρ for $n = 10, 20, 30$ and 40 .

values of n . We see that $\mu(\rho)$ monotonically increases with ρ , whereas $\nu(\rho)$ first increases and then decreases with ρ . Hence, for each $\Lambda < \Theta(n) + D(n)$ there will be a unique ρ such that $\mu(\rho) = \Lambda$. We shall take this ρ to be the operating occupancy of a node corresponding to the arrival rate λ packet per second into each node, i.e., for each n , we take $\rho = \mu^{-1}(\Lambda)$.

Now with the above approximation we can easily obtain various performance measures.

Aggregate throughput: The aggregate throughput of the network with n nodes can be obtained as

$$\Phi(n, \Lambda) = \nu(n, \mu^{-1}(\Lambda))$$

Note that, for $\Lambda \geq \Theta(n) + D(n)$, $\Phi(n, \Lambda) = \Theta(n)$.

Mean Sojourn time: As per the approximation made, each packet is discarded with probability $P_{discard}$ independently of anything else. Hence we can view each node’s queue as having two independent Poisson arrival processes with rates $\lambda P_{discard}$ and $\lambda(1 - P_{discard})$. Assuming an M/M/1 model (i.e., an exponential approximation for the service time) we obtain the data packet mean sojourn time

$$\Delta(n, \Lambda) = \left(\frac{\mu^{-1}(\Lambda)}{1 - \mu^{-1}(\Lambda)} \right) \frac{1}{\lambda}$$

Using an M/G/1 model a more exact sojourn time analysis can be done; however, this requires both first and second moments of the packet service time.

Discard probability: The discard probability is approximately

$$P_{discard}(n, \Lambda) = (\Lambda - \nu(n, \mu^{-1}(\Lambda))) / \Lambda$$

Observations: Figures 21 and 22 show the analytical as well as ns2 simulation results for 20 and 40 node networks, respectively. The plots show that the analysis is able to capture

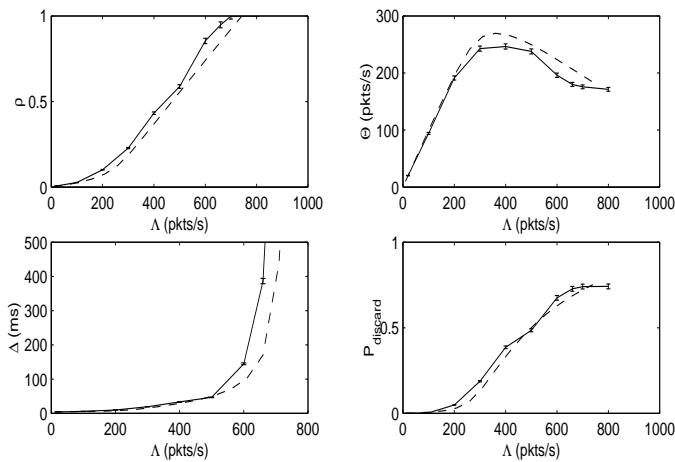


Fig. 21. Analysis and simulation plots for $n = 20$ with default parameters, and Poisson arrivals. The solid lines shown simulation results, and the dashed lines show analysis results. Simulation results show 95% confidence intervals.

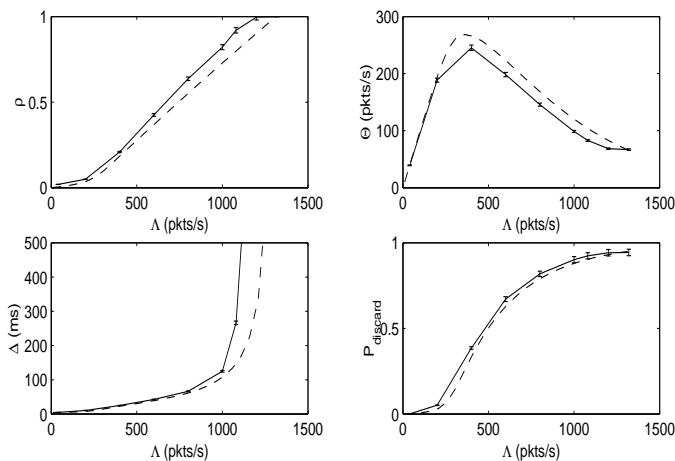


Fig. 22. Analysis and simulation plots for $n = 40$ with default parameters, and Poisson arrivals. The solid lines shown simulation results, and the dashed lines show analysis results. Simulation results show 95% confidence intervals.

the trends of all the performance measures very well in all the cases, and the values ρ , Θ , and $P_{discard}$ are approximated very well. The following observations can be made:

- We notice that for small Λ the discard probability is small and the aggregate throughput, Θ , increases with Λ , until Θ peaks and then drops down to the saturation throughput (which can be read off, for each n , from Figure 16). Thus with finite load more throughput can be sustained than the saturation throughput. The reason for this can be seen from Figure 16. Consider the 40 nodes case in Figure 22. The saturation throughput for 40 nodes, from Figure 16, is the same as the value to which Θ drops in Figure 22, when Λ becomes large. When Λ is small, however, ρ is small, thus only a small number of nodes contend at a time, and, as seen from Figure 16, the throughput can be much larger.
- Notice that, in both examples, as Λ increases ρ increases. Eventually ρ approaches 1, i.e., the nodes become saturated. At this point, for each value of n , 20 or 40, the

values of Θ , and $P_{discard}$ are the same as those shown in Figure 16, as would be expected.

- For measurement and control applications, it appears that the discard probability will determine the capacity. Consider, for example, Figure 22. If the target mean delay is 50ms, then an arrival rate of $\Lambda = 700$ pkts/sec can be sustained. However, this gives a discard probability greater than 50%! For a reasonable discard rate, the value of Λ can be no more than 200 pkts/sec.
- The mean delay approximation works well in the region of delay performance that the network would be engineered for. Thus the approximate analysis is adequate for practical network engineering.

IX. NODE LIFETIME ANALYSIS

In this section, we use the analytical model developed earlier to estimate the lifetime of a sensor node in a star topology network. We assume that the PAN-coordinator is supplied line power; hence the power consumed by the PAN-coordinator is not an issue. The network lifetime is determined by the lifetime of the leaf nodes, which are battery powered. We analyse the energy consumed by the RF transceiver in a node. The currents drawn by the other devices in a sensor node implementation are not considered, under the assumption that the communication component draws the predominantly larger current. We define the lifetime of a node as the expected lifetime assuming that the other nodes continue to work throughout the life of the node.

A. RF Transceiver Parameters

It is assumed that the sensor nodes use an RF transceiver based on the Chipcon CC2420 chip [6]. The nodes are powered by two AA batteries. These devices need a supply voltage in the range 3.1 V to 2.1 V [6]. The batteries are used in series, and we assume that both are rated at 2000mAh down to 1.05 V. We use the following information from the chipcon CC2240 data sheet [6]:

- The current drawn while a node is sleeping is $I_{idle} = 0.426$ mA.
- The current consumption of the chip in receive mode is a constant $I_{rcv} = 18.8$ mA
- The receiver sensitivity is -94 dBm.
- The transmission power in the nodes can be programmed from -25 dBm to 0 dBm in steps. The currents drawn corresponding to the different transmission powers is shown in Table II.

Transmission Power (dBm)	Current (mA)
-25	8.5
-15	9.9
-10	11
-5	14
0	17.4

TABLE II

BATTERY CURRENT CORRESPONDING TO DIFFERENT TRANSMISSION POWERS FOR THE CHIPCON CC2240 TRANSCEIVER.

It can be shown that, given the above receiver sensitivity, a transmit power of -15 dBm is required for a 10 m radius network, with path loss exponent $\eta = 2$, thus needing a transmit current $I_{txmit} = 9.9$ mA.

B. Time Average Current Drawn by a Node Transceiver

Our analytical approach is to determine the time average current (in mA) drawn by a node, assuming that all the other nodes function indefinitely. Dividing the battery capacity (in mAh) by this time average current yields an estimate of the node lifetime. We will write the time average current in terms of the following quantities that can be derived from our earlier analysis (as we will show below). The number of nodes is fixed at n , and the aggregate arrival process is Poisson with Λ (equally distributed over the nodes); these parameters are implicit in the following notation.

$r_{data-ack}$:= the rate of successful transmissions by a node

r_{CCA} := the rate at which a node performs CCAs

r_{coll} := the rate of a node experiencing collisions

T_{data} := the radio time for successful transmission of a data packet (= $(42 \times 8 \text{ bits})/250\text{kbps} = 1.34 \text{ ms}$)

T_{ack} := the time taken for the reception of an ACK packet = $384 \mu\text{s}$

T_{CCA} := the time taken for performing a CCA = 8 symbol times = $128 \mu\text{s}$

T_{coll} := the radio time for transmission by a node during a collision = $(42 \times 8 \text{ bits})/250\text{kbps} = 1.34 \text{ ms}$

α_f := the probability that a CCA by a node fails

α_{fcoll} := the probability that the node finds the channel in a collision

α_{fCCA1} := the probability that the CCA 1 by a node coincides with the CCA 1 of another node

$\alpha_{fdata-ack^*}$:= the probability that the CCA 1 by a node overlaps with a time $T_{data-ack^*}$ (see Section V-A)

In the above notation, the probabilities with subscripts of the form $f\dots$ refer to the fact that we are dealing the finite load case here. We find α_{fCCA1} , α_f , $\alpha_{fdata-ack^*}$ and α_{fcoll} as follows (where, as in Section VIII, ρ is the fraction of time a node has nonempty queues, and hence is contending; and

$$B(\rho, (n-1); m) := \binom{n-1}{m} \rho^m (1-\rho)^{(n-1)-m}$$

$$\alpha_{fCCA1} = \sum_{m=1}^{n-1} B(\rho, (n-1); m) (\alpha_{CCA1}(m))$$

$$\alpha_f = \sum_{m=1}^{n-1} B(\rho, (n-1); m) (\alpha(m))$$

$$\alpha_{fdata-ack^*} = \sum_{m=1}^{n-1} B(\rho, (n-1); m) (\alpha_{data-ack^*}(m))$$

$$\alpha_{fcoll} = \sum_{m=1}^{n-1} B(\rho, (n-1); m) (\alpha_{coll}(m))$$

where the argument (m) denotes the corresponding probabilities for the m node saturated case.

Then the time average current (in mA) drawn from the battery

$$\begin{aligned} I_{av} = & r_{data-ack} (I_{txmit} T_{data} + I_{rcv} T_{ack}) + r_{coll} I_{txmit} T_{coll} \\ & + r_{CCA} I_{rcv} T_{CCA} (2 - (\alpha_{fdata-ack^*} + \alpha_{fcoll})) \\ & + I_{idle} (1 - [r_{data-ack} (T_{data} + T_{ack}) + r_{coll} T_{coll} \\ & + r_{CCA} T_{CCA} (2 - (\alpha_{fdata-ack^*} + \alpha_{fcoll}))]) \end{aligned}$$

The terms in the above equation are explained and derived as follows.

Given an arrival rate Λ (as in Section VIII) the rate at which a node transmits packets is $r_{data-ack} = \frac{1}{n} \nu(n, \mu^{-1}(\Lambda))$. Associated with each of these transmissions, the node transmits for a time T_{data} consuming current I_{txmit} and receives an ACK for a time T_{ack} using current I_{rcv} . So the time average current consumed for this is given by $r_{data-ack} (I_{txmit} T_{data} + I_{rcv} T_{ack})$.

We next turn to deriving r_{CCA} . As explained earlier (see Section V-D), when a node has packets, it can be viewed as going through cycles, each of which starts at the end of a node activity (success or collision) (see Figure 14). In a cycle there are several failed CCAs (and perhaps even dropped packets), followed by either a success, a collision. Denote by β_f the attempt rate of a node (per backoff period) during the times when it is performing backoffs (here again the subscript f means that we are dealing with the finite load case). We compute β_f as follows

$$\beta_f = G(\alpha_f, \alpha_{fdata-ack^*}, \alpha_{fcoll})$$

where $G(\cdot, \cdot, \cdot)$ is as defined in Section V-D. For the j th such cycle, let Y_j denote the number of CCAs performed by the node, and let Z_j denote the cycle length. Then

$$r_{CCA} = \rho \frac{EY}{EZ}$$

where ρ captures the fraction of time that the node has packets, and hence is contending. Since a CCA fails with probability α_f , we obtain the following equation for EY , using a renewal argument

$$EY = \beta_f (1 + \alpha_f EY + (1 - \alpha_f) \cdot 0) + (1 - \beta_f) EY$$

This equation is understood as follows. After a backoff period, a node attempts (i.e., does a CCA) with probability β_f . The CCA fails with probability α_f and the remaining mean number of CCAs is again EY . This yields

$$EY = \frac{\beta_f}{1 - (1 - \beta_f) - \beta_f \alpha_f}$$

In a similar fashion we obtain the equation (denoting by δ the backoff period duration)

$$\begin{aligned} EZ = & \delta + (1 - \beta_f) EZ + \beta_f \alpha_f EZ + \beta_f \alpha_{fCCA1} T_{coll} \\ & + \beta_f (1 - (\alpha_f + \alpha_{fCCA1})) (T_{data-ack} + \delta) \end{aligned}$$

where we note that with probability α_{fCCA1} the node's CCA1 overlaps with another CCA1, thus leading to a collision. Solving this equation yields

$$EZ = \frac{\delta + \beta_f (1 - (\alpha_f + \alpha_{fCCA1})) (T_{data-ack} + \delta) + \beta_f \alpha_{fCCA1} T_{coll}}{1 - (1 - \beta_f) - \beta_f \alpha_f}$$

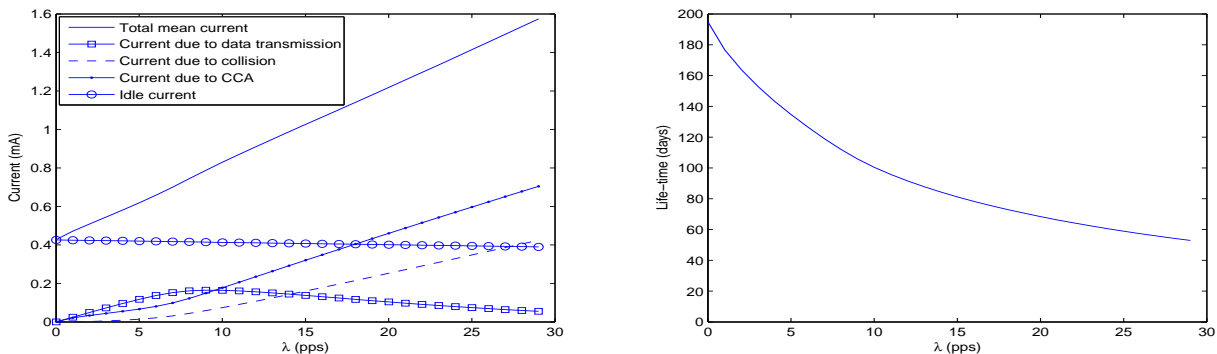


Fig. 23. Average currents (mA) (left), and mean node lifetime (days) (right) obtained from analysis vs. per node arrival rate; 40 nodes; star topology.

Thus, finally, we obtain

$$r_{CCA} = \rho \frac{EY}{EZ} = \frac{\beta_f}{\rho \delta + \beta_f(1 - (\alpha_f + \alpha_{fCCA1}))(T_{data-ack} + \delta) + \beta_f \alpha_{fCCA1} T_{coll}}$$

A CCA1 succeeds with probability $(1 - (\alpha_{fdata-ack} + \alpha_{fcoll}))$. If a CCA1 succeeds, a CCA2 is performed. So the time average current consumed by CCAs is given by $r_{CCA} I_{rcv} T_{CCA} (2 - (\alpha_{fdata-ack} + \alpha_{fcoll}))$.

In a similar way, the rate of collisions can be seen to be

$$\begin{aligned} r_{coll} &= \rho \frac{\alpha_{fCCA1}}{(1 - (\alpha_f + \alpha_{fCCA1}) + \alpha_{fCCA1})EZ} \\ &= \rho \frac{\alpha_{fCCA1}}{(1 - \alpha_f)EZ} \end{aligned}$$

So the current drawn by collisions is $r_{coll} I_{txmit} T_{coll}$.

Finally, during the remaining time the node draws the current I_{idle} . Thus, all the terms in the above equation for I_{av} are explained.

C. Expected Node Lifetime

The lifetime of a node that uses 2000 mAh batteries in series can be obtained as

$$\text{Mean Lifetime} = \frac{2000}{I_{av}} \text{ hours}$$

In Figure 23 we plot the average currents, and mean lifetime obtained from this approach, versus the arrival rate per node for a 40 node star topology. When the packet arrival rate is 0, the only power consumption is due to idle current, i.e., 0.426 mA. So the idle lifetime is $\frac{2000mAh}{0.426mA} = 195.6$ days. When the packet arrival rate increases, the current consumption increases, and the lifetime decreases to about 50 days with an arrival rate of 29 packets per second per node. Observe that the CCA sensing current and the collision current both increase with the arrival rate, whereas the current used in data transmission increases and then decreases. The decrease in the current used for data transmission relates to the behaviour of $\nu(\rho)$ shown in Figure 20; at higher arrival rates more packets get dropped and throughput decreases. Notice also that the average idle current decreases only slightly, indicating that the RF transceiver is active for only a small fraction of the time.

Now turning to Figure 22, if for desired QoS the network is operated at 200 packets per second, or 5 packets per second per node, we have a node lifetime of about 135 days.

X. SUMMARY

We summarise here some insights gained from our analysis.

- With saturated nodes, the CSMA/CA channel in the IEEE 802.15.4 MAC standard has a cyclical evolution that can be effectively modeled by a Markov renewal process. We obtained this result as a consequence of our detailed identification of the various node interaction scenarios that arise.
- The saturation analysis was found to yield a very effective heuristic for carrying out a finite arrival rate analysis. A variety of performance measured were estimated very well.
- The default back-off parameters are such that the node attempt rate levels off with increasing number of nodes, and the saturation throughput drops sharply. Our model showed that the attempt probability needed to be substantially reduced, which was achieved by simple back-off parameter adjustments.
- Even though the saturation throughput drops with the number of nodes, the network can operate at a much higher finite arrival rate provided the node occupancy, ρ , at this rate stays small.

The following network engineering insights were obtained.

- For measurement and control applications, the capacity of the network (with the default parameters) can be expected to be $P_{discard}$ limited.
- Our analytical model yields various rates and probabilities from which a simple node lifetime analysis can be derived.
- The ns-2 simulations are very time consuming. For 40 or 50 nodes even a single run for a single value of arrival rate takes 6 to 8 hours. Our analytical model has yielded very accurate results and hence can be very useful in a network engineering process.

In other work, we have extended our analysis to multihop topologies with one or more beaconing devices.

REFERENCES

- [1] IEEE std. 802.15.4, "Part 15.4: Wireless MAC and PHY specifications for Low-Rate Wireless Personal Area Networks", May 2003.
- [2] ZigBee Alliance, "Draft standard: 02130r4ZB-NWK-Network layer specification", March, 2003.
- [3] P.M. Ameer, "Analysis of Zigbee Network Architectures for Industrial Sensor Networks," *Master of Engg. Thesis, ECE Dept., Indian Institute of Science, Bangalore, June 2006*.
- [4] G. Bianchi, "Performance analysis of the IEEE 802.11 Distributed Coordination Function", *IEEE JSAC, vol. 18, no. 3, pp. 535-547, March 2000*.
- [5] Ed Callaway, P. Gorday, L. Hester, J. A. Gutierrez, M. Neave, B. Heile, V. Bahl, "Home Networking with 802.15.4: A developing standard for low-rate wireless personal area networks", *IEEE Communication Magazine, vol. 40, no. 8, pp. 70-77, August 2002*.
- [6] Chipcon Data Sheet for CC2420 2.4 GHz IEEE 802.15.4/ZigBee RF Transceiver, 2004., http://www.chipcon.com/files/CC2420_Data_Sheet_1_3.pdf
- [7] N. Golmie, D. Cypher, O. Rebal, "Performance Analysis of Low Rate Wireless Technologies For Medical Applications", *Elsevier Comp. and Commun., vol. 28, no. 10, pp. 1266-1275, June 2005*.
- [8] Munish Goyal, "Stochastic Control of Wireless Transmissions over Multiaccess Fading Channels", *Phd. Thesis, IISc, Dec. 2003*.
- [9] Patrick Kinney, "ZigBee Technology: Wireless Control that Simply Works", *Communication Design Conference, October 2003*.
- [10] Anurag Kumar, Eitan Altman, Daniele Miorandi and Munish Goyal, "New Insights from a Fixed Point Analysis of Single Cell IEEE 802.11 WLANs", *IEEE INFOCOM, vol.3, pp. 1550-1561, March 2005*. Also to appear in IEEE Transactions on Networking 2007.
- [11] Jianliang Zheng and Myung J. Lee, "Will IEEE 802.15.4 Make Ubiquitous Networking a Reality?— A Discussion on a Potential Low Power, Low Bit Rate Standard", *IEEE Communications Magazine, vol. 42, no. 6, pp. 140-146, June 2004*.
- [12] Gang Lu, Bhaskar Krishnamachari, Cauligi S. Raghavendra, "Performance Evaluation of the IEEE 802.15.4 MAC for Low-Rate Low-Power Wireless Networks", *IEEE IPCCC, pp. 701-706, April 2004*.
- [13] N.F. Timmons and W.G. Scanlon, "Analysis of the Performance of IEEE 802.15.4 for Medical Sensor Body Area Networking", *IEEE SECON 04, pp. 16-24, October 2004*.
- [14] Jianliang Zheng, "[ns] 802.15.4 source code", <http://ees2cy.engr.cuny.cuny.edu/zheng/pub/index.html>
- [15] Jianliang Zheng and Myung J. Lee, "A comprehensive Performance Study of IEEE 802.15.4", *Sensor Network Operations, IEEE Press, Wiley Interscience, Chapter 4, pp. 218-237, 2006*.
- [16] Mikko Kohvakka, Mauri Kuorilehto, Marko Hannikainen, Timo D. Hamalainen, "Performance Analysis of IEEE 802.15.4 and ZigBee for Large-Scale Wireless Sensor Network Applications", *ACM PE-WASUN, pp. 48-57, October 2006*.
- [17] Jelena Mistic, Shairmina Shafi, Vojislav B. Mistic, "Performance of a Beacon Enabled IEEE 802.15.4 Cluster with Downlink and Uplink Traffic", *IEEE Transactions on Parallel and Distributed Systems, vol. 17, no. 4, pp. 361-376, April 2006*.
- [18] Sofie Pollin, Mustafa Ergen, Sinem Coleri Ergen, Bruno Bougard, Liesbet Van der Perre, Francky Catthoor, Ingrid Moerman, Ahmad Bahai, Pravin Varaiya, "Performance Analysis of Slotted Carrier Sense IEEE 802.15.4 Medium Access Layer", *IEEE GLOBECOM, pp. 1-6, Nov. 2006*.
- [19] T. R. Park, T. H. Kim, J. Y. Choi, S. Choi, W. H. Kwon, "Throughput and Energy Consumption Analysis of IEEE 802.15.4 Slotted CSMA/CA", *Electronic Letters, vol. 41, no.18, pp. 1017-1019, Sept. 2005*.
- [20] Kenji Leibnitz, Naoki Wakamiya, and Masayuki Murata, "Modeling of IEEE 802.15.4 in a Cluster of Synchronized Sensor Nodes", *ITC 19, pp. 1345-1354, Aug.-Sept. 2005*.
- [21] Zhifeng Tao, Panwar S., Daqing Gu, Jinyun Zhang, "Performance Analysis and a Proposed Improvement for the IEEE 802.15.4 Contention Access Period", *IEEE WCNC, vol. 4, pp. 1811- 1818, April 2006*.
- [22] Iyappan Ramachandran, Arindam K. Das and Sumit Roy, "Analysis of the Contention Access Period of IEEE 802.15.4 MAC", *ACM TOSN, vol. 3, no. 1, article 4, March 2007*.
- [23] Iyappan Ramachandran, "Changes made to the IEEE 802.15.4 NS-2 Implementation", http://www.ee.washington.edu/research/funlab/802_15_4/ns2_changes.pdf
- [24] Anis Koubaa, Mario Alves, Eduardo Tovar, "i-GAME: AN Implicit GTS Allocation Mechanism in IEEE 802.15.4 for Time-Sensitive Wireless Sensor Networks", *IEEE ECRTS, pp. 10-19, July 2006*.
- [25] Anis Koubaa, Mario Alves, Eduardo Tovar, "A Comprehensive Simulation Study of Slotted CSMA/CA for IEEE 802.15.4 Wireless Sensor Networks", *IEEE WFCS, pp. 183-192, June 2006*.

APPENDIX

A. ANALYSIS OF THE THE CHANNEL EVOLUTION MRP

We see that in the Markov renewal process formulated in Section V-A, the only feasible possibilities for (U_i, X_i) are $\{(T_{coll} + j\delta, k), j = 2, 3, \dots, J; k = 1, 2, \dots, n-2; (T_{data-ack} + 2\delta, n-1), (T_{coll} + (J+1)\delta, n), (\delta, n)\}$. Using the decoupling approximation of Section V-C, the transition probabilities for the process can be obtained as follows.

A. Transition probabilities for the MRP

1) $X_i = n$ i.e., this cycle starts with any of the nodes being available to attempt.

a) $(U_{i+1}, X_{i+1}) = (\delta, n)$, if none of the n nodes attempts. Thus,

$$P(U_{i+1} = \delta, X_{i+1} = n | X_i = n) = (1 - \beta)^n$$

b) $(U_{i+1}, X_{i+1}) = (T_{data-ack} + 2\delta, n-1)$, if exactly one of the n nodes attempts. Thus,

$$P(U_{i+1} = T_{data-ack} + 2\delta, X_{i+1} = n-1 | X_i = n) = n\beta(1 - \beta)^{(n-1)}$$

c) $(U_{i+1}, X_{i+1}) = (T_{coll} + j\delta, k_2)$, if exactly $n - k_2 (\geq 2)$ out of n nodes attempt. Further none of the remaining k_2 nodes attempts for $(j - 2)$ backoff periods after the collision, and at least one of them attempts in the very next backoff period. Thus, for $1 \leq k_2 \leq n - 2, 2 \leq j \leq J$,

$$P(U_{i+1} = T_{coll} + j\delta, X_{i+1} = k_2 | X_i = n) = \binom{n}{n - k_2} \beta^{n-k_2} (1 - \beta)^{k_2} ((1 - \beta)^{k_2})^{(j-2)} (1 - (1 - \beta)^{k_2})$$

d) $(U_{i+1}, X_{i+1}) = (T_{coll} + (J+1)\delta, n)$, if $k, 2 \leq k \leq n$, nodes attempt, and none of the remaining $n - k$ nodes attempts for $(J - 1)$ consecutive backoff periods after collision in this cycle. Thus,

$$P(U_{i+1} = T_{coll} + (J+1)\delta, X_{i+1} = n | X_i = n) = \sum_{k=2}^n \binom{n}{k} \beta^k (1 - \beta)^{(n-k)} ((1 - \beta)^{(n-k)})^{(J-1)}$$

It can be checked that

$$\sum_{u,x} P(U_{i+1} = u, X_{i+1} = x | X_i = n) = 1$$

since

$$\begin{aligned} & (1 - \beta)^n + n\beta(1 - \beta)^{(n-1)} \\ & + \sum_{j=2}^J \sum_{k_2=1}^{n-2} \binom{n}{n - k_2} \beta^{n-k_2} (1 - \beta)^{k_2} ((1 - \beta)^{k_2})^{(j-2)} (1 - (1 - \beta)^{k_2}) \\ & + \sum_{k=2}^n \binom{n}{k} \beta^k (1 - \beta)^{(n-k)} ((1 - \beta)^{(n-k)})^{(J-1)} = 1 \end{aligned}$$

2) $X_i = n - 1$ i.e., this cycle starts with $(n - 1)$ of the nodes being available to attempt. This is similar to the case $X_i = n$.

a) $(U_{i+1}, X_{i+1}) = (\delta, n)$, if none of the $n - 1$ nodes attempts. Thus,

$$P(U_{i+1} = \delta, X_{i+1} = n | X_i = n - 1) = (1 - \beta)^{n-1}$$

b) $(U_{i+1}, X_{i+1}) = (T_{data-ack} + 2\delta, n - 1)$, if exactly one of the $n - 1$ nodes attempts. Note that the node that was not included at the start of the cycle would be ready to attempt at the end of the cycle, whether one of the other nodes would not be able to attempt. Thus,

$$P(U_{i+1} = T_{data-ack} + 2\delta, X_{i+1} = n - 1 | X_i = n - 1) = (n - 1)\beta(1 - \beta)^{(n-2)}$$

c) $(U_{i+1}, X_{i+1}) = (T_{coll} + j\delta, k_2)$, if exactly $n - k_2 (\geq 2)$ out of $n - 1$ nodes attempt. Further none of the remaining k_2 nodes attempt for $(j - 2)$ backoff periods after the collision, and at least one of them attempts in the the very

next backoff period. We note here that the node that is not available to attempt at the beginning of the cycle, can attempt after $T_{coll} + 2\delta$ and is included in the calculation. Thus, for $1 \leq k_2 \leq n-2, 2 \leq j \leq J$,

$$P(U_{i+1} = T_{coll} + j\delta, X_{i+1} = k_2 | X_i = n-1) = \binom{n-1}{n-k_2} \beta^{n-k_2} (1-\beta)^{(k_2-1)} ((1-\beta)^{k_2})^{(j-2)} (1 - (1-\beta)^{k_2})$$

- d) $(U_{i+1}, X_{i+1}) = (T_{coll} + (J+1)\delta, n)$, if $k, 2 \leq k \leq n-1$, nodes attempt, and none of the remaining $n-k$ nodes attempts for $(J-1)$ consecutive backoff periods after collision in this cycle. Thus,

$$P(U_{i+1} = T_{coll} + j\delta, X_{i+1} = n | X_i = n-1) = \sum_{k=2}^{(n-1)} \binom{n-1}{k} \beta^k (1-\beta)^{(n-1-k)} ((1-\beta)^{(n-k)})^{(J-1)}$$

As in case 1, it can be checked that

$$\sum_{u,x} P(U_{i+1} = u, X_{i+1} = x | X_i = n-1) = 1$$

since

$$\begin{aligned} & (1-\beta)^{(n-1)} + (n-1)\beta(1-\beta)^{(n-2)} \\ & + \sum_{j=2}^J \sum_{k_2=1}^{n-2} \binom{n-1}{n-k_2} \beta^{n-k_2} (1-\beta)^{k_2} ((1-\beta)^{k_2})^{(j-2)} (1 - (1-\beta)^{k_2}) \\ & + \sum_{k=2}^{(n-1)} \binom{n-1}{k} \beta^k (1-\beta)^{(n-1-k)} ((1-\beta)^{(n-k)})^{(J-1)} = 1 \end{aligned}$$

- 3) Consider $k_1 \in \{1, 2, \dots, n-2\}, k_2 \in \{1, 2, \dots, n-2\}, j \in \{2, 3, 4\}$. If $X_i = k_1$ i.e., this cycle starts with k_1 of the nodes being available to attempt. It itself implies that one of them has attempted.

- a) $(U_{i+1}, X_{i+1}) \neq (\delta, n)$, because at least one of the k_1 nodes has attempted, and the cycle cannot be an idle one. Thus,

$$P(U_{i+1} = \delta, X_{i+1} = n | X_i = k_1) = 0$$

- b) $(U_{i+1}, X_{i+1}) = (T_{data-ack} + 2\delta, n-1)$, if exactly one of the k_1 nodes attempts, given that at least one of them has attempted. Thus,

$$P(U_{i+1} = T_{data-ack} + 2\delta, X_{i+1} = n-1 | X_i = k_1) = \frac{k_1 \beta (1-\beta)^{(k_1-1)}}{1 - (1-\beta)^{k_1}}$$

- c) $(U_{i+1}, X_{i+1}) = (T_{coll} + j\delta, k_2)$, if exactly $n-k_2 (\geq 2)$ of k_1 contending nodes attempt ($n-k_2 \leq k_1$). To ensure the following cycle length to be $(2\delta + T_{coll} + (j-2)\delta)$, it is necessary that none of the k_2 nodes attempts during first $(j-2)$ backoff periods after collision but at least one of them attempts in the very next backoff period. The next state cannot be $(T_{coll} + j\delta, k_2)$, if $n-k_2 > k_1$. As we have already discussed availability of less than $n-1$ nodes itself implies that at least one of them has attempted. Thus,

$$P(U_{i+1} = T_{coll} + j\delta, X_{i+1} = k_2 | X_i = k_1) = \frac{\binom{k_1}{n-k_2} \beta^{n-k_2} (1-\beta)^{(k_1+k_2-n)} ((1-\beta)^{(n-k_2)})^{(j-2)} (1 - (1-\beta)^{(n-k_2)})}{1 - (1-\beta)^{k_1}},$$

if $k_1 + k_2 \geq n, k_1 > 1$,

0, otherwise.

- d) $(U_{i+1}, X_{i+1}) = (T_{coll} + (J+1)\delta, n)$, if some $k, 2 \leq k \leq k_1$, nodes attempt out of the k_1 nodes available to contend. To ensure the cycle length to be $(2\delta + T_{coll} + (J-1)\delta)$, it is necessary that none of the $n-k$ nodes attempts during first $(J-1)$ backoff periods after collision. Thus,

$$P(U_{i+1} = T_{coll} + (J+1)\delta, X_{i+1} = n | X_i = k_1) = \frac{\sum_{k=2}^{k_1} \binom{k_1}{k} \beta^k (1-\beta)^{(k_1-k)} ((1-\beta)^{(n-k)})^{(J-1)}}{1 - (1-\beta)^{k_1}}, \text{ if } k_1 > 1,$$

0, otherwise.

As in cases 1 and 2, again it can be checked that for $k_1 \in \{1, 2, \dots, n-2\}$,

$$\sum_{u,x} P(U_{i+1} = u, X_{i+1} = x | X_i = k_1) = 1$$

since for $k_1 = 1$,

$$\frac{k_1 \beta (1-\beta)^{(k_1-1)}}{1 - (1-\beta)^{k_1}} = 1$$

and for $k_1 > 1$,

$$\begin{aligned} & \frac{k_1 \beta (1-\beta)^{(k_1-1)}}{1 - (1-\beta)^{k_1}} \\ & + \sum_{k_2=n-k_1}^{n-2} \frac{\binom{k_1}{n-k_2} \beta^{n-k_2} (1-\beta)^{(k_1+k_2-n)} ((1-\beta)^{(n-k_2)})^{(j-2)} (1 - (1-\beta)^{(n-k_2)})}{1 - (1-\beta)^{k_1}} \\ & + \frac{\sum_{k=2}^{k_1} \binom{k_1}{k} \beta^k (1-\beta)^{(k_1-k)} ((1-\beta)^{(n-k)})^{(J-1)}}{1 - (1-\beta)^{k_1}} = 1 \end{aligned}$$

1) *Transition Probabilities for the Channel with Single Node*: In case of a channel comprising of single node, although a successful transmission takes only 4 symbol times in the last backoff period, the node cannot attempt for its next packet in the same backoff period. Hence a successful transmission consumes effectively $T_{data-ack} + 3\delta$ time. A backoff period will be an idle cycle, if the node is in backoff and doesnot attempt in that backoff period. There cannot be any collisions. Hence, only feasible possibilities for (U_i, X_i) are $(T_{data-ack} + 3\delta, 1)$ and $(\delta, 1)$. Transition probabilities for the Markov renewal process can be obtained as follows.

- $X_i = 1 \forall i$

1) $(U_{i+1}, X_{i+1}) = (\delta, 1)$, if the node doesnot attempt. Thus,

$$P(U_{i+1} = \delta, X_{i+1} = 1 | X_i = 1) = 1 - \beta$$

2) $(U_{i+1}, X_{i+1}) = (T_{data-ack} + 3\delta, 1)$, if the node attempts. Thus,

$$P(U_{i+1} = T_{data-ack} + 3\delta, X_{i+1} = 1 | X_i = 1) = \beta$$

B. Transition Probabilities for the Markov Chain $\{X_i, i \geq 0\}$

Let \mathbf{M} be the transition probability matrix for the one dimensional Markov chain $\{X_i, i \geq 0\}$.

For $k_1, k_2 = 1, 2, 3, \dots, n-2$;

$$M_{k_1, k_2} = \sum_{j=2}^J P(U_{i+1} = T_{coll} + j\delta, X_{i+1} = k_2 | X_i = k_1)$$

$$M_{k_1, n-1} = P(U_{i+1} = T_{data-ack} + 2\delta, X_{i+1} = n-1 | X_i = k_1)$$

$$M_{k_1, n} = P(U_{i+1} = T_{coll} + (J+1)\delta, X_{i+1} = n | X_i = k_1) \\ + P(U_{i+1} = \delta, X_{i+1} = n | X_i = k_1)$$

$$M_{n-1, k_2} = \sum_{j=2}^J P(U_{i+1} = T_{coll} + j\delta, X_{i+1} = k_2 | X_i = n-1)$$

$$M_{n-1, n-1} = P(U_{i+1} = T_{data-ack} + 2\delta, X_{i+1} = n-1 | X_i = n-1)$$

$$M_{n-1, n} = P(U_{i+1} = T_{coll} + (J+1)\delta, X_{i+1} = n | X_i = n-1) \\ + P(U_{i+1} = \delta, X_{i+1} = n | X_i = n-1)$$

$$M_{n, k_2} = \sum_{j=2}^J P(U_{i+1} = T_{coll} + j\delta, X_{i+1} = k_2 | X_i = n)$$

$$M_{n, n-1} = P(U_{i+1} = T_{data-ack} + 2\delta, X_{i+1} = n-1 | X_i = n)$$

$$M_{n, n} = P(U_{i+1} = T_{coll} + (J+1)\delta, X_{i+1} = n | X_i = n) \\ + P(U_{i+1} = \delta, X_{i+1} = n | X_i = n)$$

C. Conditional Distribution of the Cycle Times

The conditional distribution of the cycle length U_{i+1} , given X_i , can be obtained as follows.

For $k_1 = 1, 2, \dots, n, j = 2, 3, \dots, J$

$$P(U_{i+1} = T_{coll} + j\delta | X_i = k_1) = \sum_{k_2=1}^{n-2} P(U_{i+1} = T_{coll} + j\delta, X_{i+1} = k_2 | X_i = k_1)$$

$$P(U_{i+1} = T_{coll} + (J+1)\delta | X_i = k_1) = P(U_{i+1} = T_{coll} + (J+1)\delta, X_{i+1} = n | X_i = k_1)$$

$$P(U_{i+1} = T_{data-ack} + 2\delta | X_i = k_1) = P(U_{i+1} = T_{data-ack} + 2\delta, X_{i+1} = n-1 | X_i = k_1)$$

$$P(U_{i+1} = \delta | X_i = k_1) = P(U_{i+1} = \delta, X_{i+1} = n | X_i = k_1)$$